

Sesam, toward a Mature Magmatic Arc Sourced from Tholeiitic Volcanisms and Calc-Alkaline Volcanoplutonism within Kedougou-Kenieba Inlier, South-East Senegal/West Africa

Mame Codou Ndiaye^{1*}, Mamadou Ndiaye², Papa Malick Ngom², Mababa Diagne³, Andrea Moscariello⁴, Antoine De Haller⁴

¹National Superior School of Mines et and Geology, Cheikh Anta Diop University, Dakar, Senegal

²Geology Department, Faculty of Sciences and Technics, Cheikh Anta Diop University, Dakar, Senegal

³Department of Earth Sciences and Environment, Amadou Makhtar Mbow University, Diamniadio, Senegal

⁴Department of Earth Sciences and Environment, University of Genova, Genova, Switzerland

Email: *mamecodou1.ndiaye@ucad.edu.sn, lalinguere100@yahoo.fr

How to cite this paper: Ndiaye, M. C., Ndiaye, M., Ngom, P. M., Diagne, M., Moscariello, A., & Haller, A. D. (2025). Sesam, toward a Mature Magmatic Arc Sourced from Tholeiitic Volcanisms and Calc-Alkaline Volcanoplutonism within Kedougou-Kenieba Inlier, South-East Senegal/West Africa. *Journal of Geoscience and Environment Protection*, 13, 331-386.

<https://doi.org/10.4236/gep.2025.131018>

Received: August 2, 2024

Accepted: January 23, 2025

Published: January 26, 2025

Copyright © 2025 by author(s) and Scientific Research Publishing Inc. This work is licensed under the Creative Commons Attribution International License (CC BY 4.0).

<http://creativecommons.org/licenses/by/4.0/>



Open Access

Abstract

The Paleoproterozoic terrains of Kedougou Inlier have an overall architecture formed of greenstones and sedimentary basins. Most of the work done on these Birimian formations has focused on either belts or basins, or even briefly on both, but more rarely on the transition zones between belts and Paleoproterozoic basins. Our study focuses on the lithostructural framework of the Mako-Diale transition zone located within the Kedougou-Kenieba Inlier. Its objective is to redefine the existing architecture. Geophysical, petrographic, structural and geochemical results from lithostructural domains allowed to building a new architecture based on three major lithostructural domains evolving into tectonomagmatic complexes associated with three shear zones corresponding to Western shear-contact (CiscoW) represented by Sabodala sinistral mylonitic shear (SSZ), to Median sinistral ductile then brittle shear-contact (CiscoM) and to Eastern dextral brittle-ductile shear-contact (CiscoE) corresponding to the Main transcurrent shear (MTZ). Tectonomagmatic complexes are represented by Maco oceanic crust, Sesam arc and Diale back-arc basin. The opening of Diale basin is related to CiscoM. Its closure set along the Faleme shear-contact (CiscoF) located beyond CiscoE. The tectonic evolution of the Eburnian orogeny within Kedougou-Kenieba inlier highlights four (4) deformations phases: CiscoW, CiscoM, CiscoE and CiscoF respectively running for D1, D2, D3 et D4. Such CiscoW along Sabodala, Sofia deposits and CiscoE along Massawa deposit, CiscoM and CiscoF stand as potential host structures for futures Kedougou inlier gold deposits. Furthermore, large plutonic masses within Mako-Diale

transition zone belong all to three (3) distinct magmatic sources: Koulountou granodiorite, Koulountou and Tinkoto granites are sourced from high-K mafic rocks; Tiguida granite and Diabba granodiorite from low-K mafic rocks, while Dioudiokoukou granite belongs to tonalite source. The Sesam arc is located along the shear corridor defined between sinistral CiscoW and sinistral CiscoM. The main lithologies consist of volcanics (andesitic breccias or agglomerates, andesitic tuffs) reworked by Tiguida and Koulountou garnet granitoids. Magmatism is marked by MORBs tholeiites associated with arc tholeiites and calc-alkaline series: tholeiites3 with MORBs affinity, tholeiites4 with MORBs affinity, arc tholeiites and calc-alkaline2 series associated with island arc. Tholeiites are associated to metaluminous, syncollisional Koulountou garnet granite and peraluminous post-collisional Tiguida garnet granite. Overall, the geodynamic evolution of the Kedougou Kenieba inlier could be linked to the single magmatic event associated with tectonomagmatic episodes. At the end of CiscoM, tectonics would have favoured the distension phase leading to the initiation of Diale back-arc basin. The plutonics and volcanics in the context of the arc must have been locally uplifted and eroded to fill Diale basin from D2 to D4 phases.

Keywords

Magmatism, Tholeiitic, Calc-Alkaline, Garnet-Granite, Sesam-Arc

1. Introduction

Birimian terrains of West African Craton are located within Baoule-Mossi domain (Man ridge), Yetti-Eglab domain (Reguibat ridge) and Kedougou-Kenieba and Kayes inliers.

The West African Craton is structured into three units: the Reguibat Ridge in the North, the Man (or Leo) Ridge in the South, and in the middle, the Kedougou-Kenieba (straddling Senegal and Mali) and Kayes inliers. Two major orogenic cycles divide the West African Craton into two domains: Archean and Paleoproterozoic.

The Archean formations are affected by two orogenic cycles: the Leonian cycle, dated between 2.9 and 2.7 Ga by Beckinsale et al. (1980), Barrere (1967) and Vachette et al. (1973) and the Liberian cycle, dated between 2.7 and 2.5 Ga by Camil et al. (1984), Barrere (1967) and Vachette et al. (1973).

Paleoproterozoic terrains are affected by two cycles: the Burkinian affecting Dabakalian terrains has been dated between 2.19 and 2.14 Ga (Tempier, 1986; Lemoine, 1988; Boher et al., 1992) and the Eburnean cycle affecting the Birimian terrains has been dated between 2.12 and 2.07 Ga (Bassot & Caen-Vachette, 1984; Feybesse et al., 1989; Abouchami et al., 1990; Liegeois et al., 1991; Boher et al., 1992; Dia et al., 1997; Hirdes et al., 1996; Gasquet et al., 2003; Pawlig et al., 2006; Gueye et al., 2007).

Most of the rich work done on these Birimian formations focuses either on the belts, on the basins or even briefly on the two associates, but more rarely on the transitional zones between volcanic belts and Paleoproterozoic basins. The stratigraphy of Kedougou Kenieba Inlier has long been debated (discussions in Vidal

et al., 1996; Baratoux et al., 2011; Kock et al., 2011; Lambert-Smith et al., 2016; Gueye et al., 2007) and seems to find a consensus with Bassot.

However, the lithostructural architecture still raises questions, in particular: the transitional zone between volcanic belt and Diale basin stand as a homogeneous or heterogeneous lithostructural framework? What are the behaviors and implications of geochemical signatures of new lithostructural framework?

This paper presents petrographic, structural, geophysical and geochemical data of the first study on upper part of Mako (transitional zone between volcanic belt and Diale basin) located between Massawa and Sofia Mines (**Figure 1**). The study defines new lithostructural architecture, highlighting a magmatic arc within Sesam tectonomagmatic domain. It constitutes a reference situation laying foundations for the redefinition of lithostructural framework of the entire Kedougou-Kenieba Inlier.

2. Objective

The aim of this study is to redefine the lithostructural architecture and geodynamic framework of the Mako-Diale transitional zone located within Kedougou Inlier. Specifically, it will involve:

- to carry out a combined petrographic, geophysical and structural study of the various formations, integrating the typology of the large plutonic masses;
- to identify the lithostructural domains, establish their boundaries and litho-tectonic characteristics;
- to define geochemical signature and its geodynamic implications in order to first, establish the typology of magmatisms and identify the relationships between magmatisms and the tectonic phases recorded within the area of study; and, second, characterise the geotectonic, geodynamic and genesis environments of the different types of magmatism identified within the Mako-Diale transitional zone.

3. Geological Context

The architecture of the paleoproterozoic formations of Man ridge (Baoule Mossi) and inliers is broadly defined as follows:

-Narrow, elongated volcanic belts, generally North-south to North-east mainly composed of basic volcanic rocks. These are known as greenstone belts. These volcanic belts show bimodal tholeiitic to calc-alkaline volcanics (Baratoux et al., 2011) and form linear greenstone belts that generally trend North-east and can extend for hundreds of kilometres.

-Basins mainly formed of sediments alternating with belts.

The belt and basin formations were deformed and metamorphosed between ~2120 Ma and ~2080 Ma during the Eburnian orogeny (Bonhomme, 1962; Oberthür 1998; Feybesse et al., 2006), during which several generations of granitoid plutons were formed.

-Granitoids account for around 70% of the Birimian terrains and form ovoid intrusions or composite batholiths ranging from tonalite-trondhjemite-granodiorite to leucogranites (Hirdes et al., 1992).

-The transition zones between belts and basins still under-studied at the scale

of West African craton. In the case study of Kegougou inlier in Senegal, the transition between belts and basins constitutes the lithostructural interface highlighting Maco, Sesam and Diabba tectonomagmatic complexes (this study).

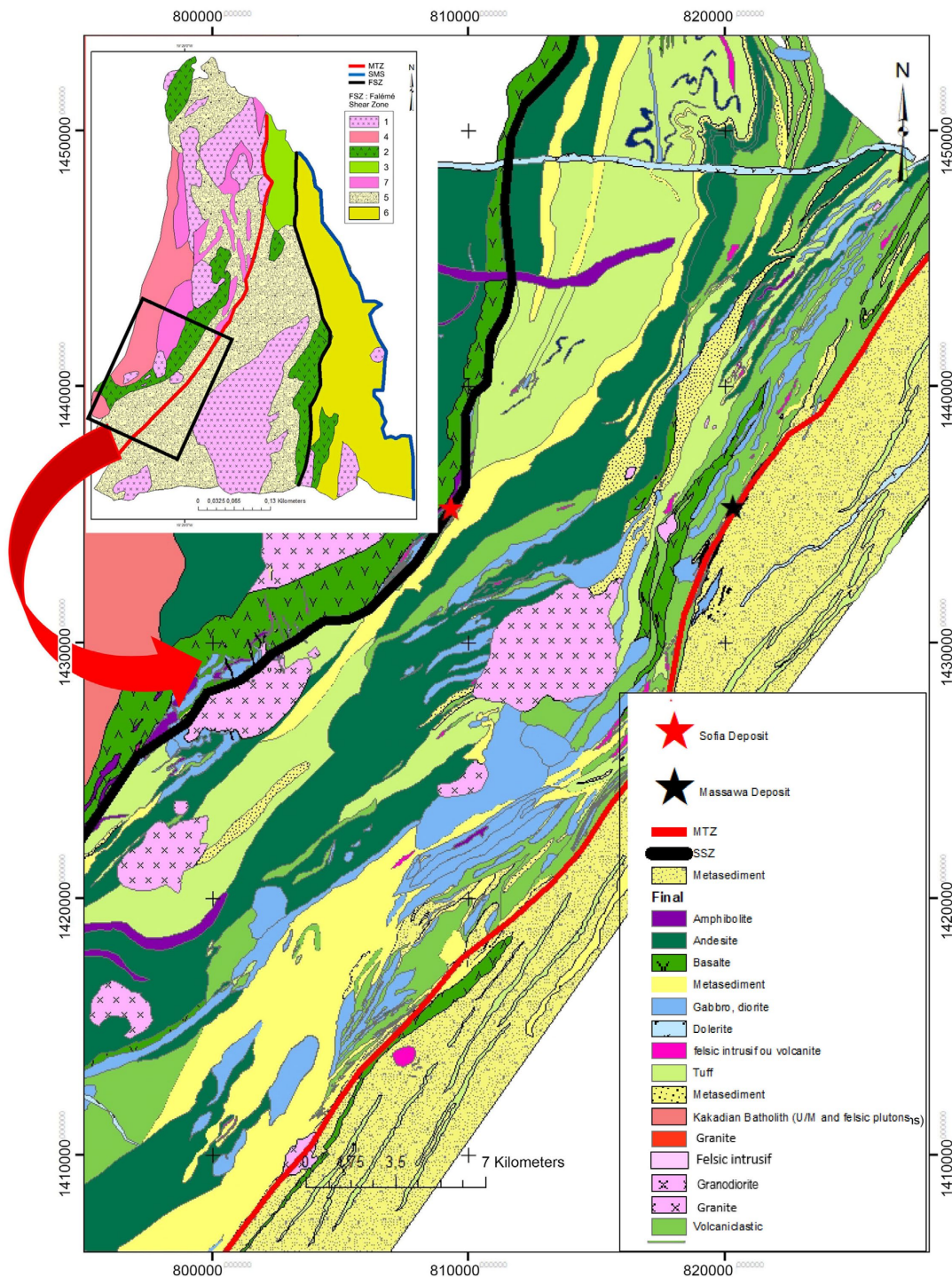


Figure 1. Location map of the area of study, geology update 2017 Randgold Ressources modified Codou (this study). On the top left regional geological map of the Kedougou Kenieba inlier (compilation Bassot, 1966 and Ledru et al., 1991 modified Codou for base map (this study); (1) large syntectonic mass, (2) and (3) volcanic, (4) batholith badon-kakadian (7), intrusive, (5) Diale Dalema and (6) Koffi.

3.1. Key Features of Transition Zones between Belts and Paleoproterozoic Basins

At the scale of West African Craton, the transition zones between greenstone belts and sedimentary basins can be observed to a large extent in Côte d'Ivoire, Burkina Faso, Niger, western Mali, Guinea, Ghana... and in Senegal.

In Burkina, the western part of the geological formations is in the form of three greenstone belts: Boromo, Hounde and Banfora generally oriented North North-east to North-south (Castaing et al., 2003; Baratoux et al., 2011; Metelka et al., 2011) associated with basins of late fine-grained sediments of Birimian age.

The transition zone between the Banfora belt and the basin is marked by the Greenville-Ferkessedougou-Bobo Dioulasso dextral shear zone (GFBSZ) intruded by synkinematic granites (Lemoine, 1988, 1990). The Boni shear marks the contact between the Hounde belt and the basin composed of late Tarkwaian' type sediments (Baratoux et al., 2011; Koffi et al., 2016). In the Boromo area, the belt/basin transition is marked by two margins: an eastern margin made up of intermediate volcanics and several ultramafic bodies, and a western margin made up of mafic bodies (basalt, pillow, orthoamphibolite/pyroxenite gabbro). A tectonically controlled basin bounded by the Ouango-Fitini shear zone to the West and the Boni shear zone to the East (Lüdtke et al., 1999).

Ivory coast the Birimian consists of volcano-sedimentary furrows that are generally oriented North-south to North-east (N020 to N050) and intercalated between granitoid batholiths. Several furrows have developed in the Dabakala region: the Haut-N'Zi, the Fettékro and the Haute Comoe. They are composed of eruptive formations, volcano-sediments and sediments. The western part of the Upper N'zi furrow is mainly covered by metasediments (Arnould, 1961). The Upper Comoe belt is an assemblage of Birimian metasedimentary and metavolcanic rocks. The contacts between volcanic belts and sedimentary basins have not yet been clearly defined, but there are numerous northeast-southwest fault structures in the northeast domain and North-south fault structures in the central part. These are interpreted as the result of two major deformations: the first is the result of tangential tectonics that produced structures oriented North-south to North-North-east, to South South-west (Feybesse et al., 1989); the second corresponds to transcurrent deformation, marked by the emplacement of large granitoid complexes around 2.1 Ga (Lemoine, 1988; Ledru, et al., 1991 in Feybesse & Milesi, 1994).

In Ghana, two-thirds of the country's surface area is dominated by Paleoproterozoic birimian formations composed of NE-trending volcanic belts separated by basins.

In the South-west of Ghana, the Birimian comprises a sequence of volcanoclastics and sediments mainly composed of fine grains and separating a series of four greenstone belts trending North-east to South-west and corresponding from West to East to the Bui, Sefwi, Ashanti and Kibi-Winneba belts. These belts are separated by three Sunyani, Kumasi and Akyem (or Cape Coast Basin) and Agyei

Duodu et al., 2009). These greenstone belts and sedimentary basins were formed and deformed during the Eburnian orogeny (Bonhomme, 1962).

The Sefwi greenstone belt is mainly composed of metamorphosed tholeiitic lavas, some volcanoclastics and synvolcanic tonalitic granitoids with granodioritic granitoids.

The centre of the Sefwi belt is largely granitoid with only minor amounts of Tarkwaian.

The Ashanti greenstone belt is one of the belts. The southern part of this belt is characterised by three volcanic lobes, consisting of basaltic flows, andesitic lavas, pyroclastic and sedimentary rocks, with an intermediate granodioritic plutonic suite. Mafic to ultramafic bodies also encroach on part of the volcanic belt. The largest mafic to ultramafic body has recently been interpreted as a paleoproterozoic ophiolite complex in the supra-subduction zone (Attoh et al., 2006).

The Sunyani-Comoe basin is intruded by numerous granitoids ranging in composition from tonalite to peraluminous granite. Zircons studied in the leucogranites immediately adjacent to the Sefwi belt give an age of 2088 ± 1 Ma (Hirdes et al., 1992 for the Kawtiago granite, Ghana). Published field studies show internal deformation microstructures with a sub-vertical foliation and a sub-horizontal stretching lineation, both parallel to their elongation direction (Vidal et al., 2009).

The Kibi-Winneba volcanic belt is located in the southeastern part of Ghana within West African Craton. It is characterised by volcanic lobes formed of basaltic flows, andesitic lavas, pyroclastic and sedimentary rocks, with granitoids occupying intermediate positions.

The Kumasi Group in the Kumasi and Akyem basins formed under an extensional regime during D2 deformation phase (stage 4 of Feybesse et al., 2006) where major faults, Ashanti and Akropong, acted as primary basin-forming structures and detachment surfaces prior to D3 reactivation.

At the transition between the basins and the volcanic belts are small outcrops of cherts, carbonates and manganese-rich sediments, which are thought to be the exhalative remains of the eruptions that formed the volcanic belts. This transition zone between the volcanic belts and the sedimentary basins is marked by chemical facies, which have been recognised as the site of much of the gold mineralisation in Ghana.

In Niger, Birimian of Liptako (NE edge of the Man Ridge) are alternating belts of green rocks and granitoid plutons trending North-east (Dupuis et al., 1991). There are three belts: Gorouol belt, Diagorou-Darbani belt and Sirba belt.

The Gorouol belt is made up of metabasites (more or less coarse metabasalts with pillow flow, metagabbros, metadolerites).

The Diagorou-Darbani belt is the central belt of the region. This belt is composed of low-grade metamorphic rocks (tholeiitic metabasalts with pillow structures) and medium-grade metamorphic rocks (garnet-amphibolites, garnet-free amphibolites and micaschists).

The Sirba belt shows metabasites (basalt, dolerite and gabbro), metavolcanoclastites (volcanic rock, tuff and cinerite) associated with metasediments (siltstone,

pelite, quartzite, greywacke, chert, conglomerate), and mainly acidic magmatic rocks (granite, granodiorite, diorite, rhyodacite, rhyolite and granophyre). The volcanic and sedimentary formations are generally metamorphosed into greenschist facies and, locally, into epidote amphibolite facies.

The Sirba basin is composed of metasediments (siltstone, pelite, quartzite, greywacke, chert, conglomerate) and magmatic rocks.

The Diagorou-Darbani basin is formed by metasediments, talcschists, chloritochists and conglomerates.

The deformation undergone by the Neoproterozoic sandstones of the Liptako (Karey Gorou, Niger) on the eastern margin of the West African Paleoproterozoic craton, is essentially materialised by a dense network of faults. Fractures due to a distensive episode, resulting from the reactivation of Mesoproterozoic fractures (around 1400 Ma) during the Pan-African cycle, and fractures linked to three Pan-african compressional phases, represented by episodes with North North-west-South South-east, West North-west to East South-east and West South-west to East North-east directions could be distinguished (Dercourt et al., 2000).

In Mali, four (4) volcanic belts (Yanfolila belt, Morila belt, Syama belt and Faleme belt) are associated with four sedimentary basins (Siguiiri basin, Bougouni-Kekoro basin, Bagoé basin and Koffi basin).

The Birimian of South-west Mali is defined by a succession of North-east to South-east oriented units (Milési et al., 1986, 1992, 2004) as a succession of greenstone belts and sedimentary basins.

There are four (4) volcanic belts: the Yanfolila belt, the Morila belt, the Syama belt and the Faleme belt.

The Yanfolila belt is around 60 km wide and contains arc-type volcanic formations, known locally as the “Nani volcanic formation,” and reworked sequences of greywackes similar to those found in the Siguiiri basin. The Yanfolila volcanic belt develops along the Yanfolila shear zone is characterised by the emplacement of basaltic rocks to the North of Yanfolila and acid pyroclastics and sediments of a sandstone-pelite nature to the South of Kangaba (Girard et al., 1998).

The Morila belt is around 50 km wide and lies along the vast Bougouni granite domain that occupies the central part of South-west Mali. The Morila Belt also contains basaltic to andesitic lavas interbedded with a suite of volcano-sedimentary formations; felsic intrusions have been dated from 2132-2097 Ma (McFarlane et al., 2011).

The Syama belt is the narrowest, about 30 km wide and lies along the Mali-Burkina Faso border. The Syama belt is broadly similar to the Yanfolila belt but is structurally much more deformed with overturned series. These different formations are intersected by plutons (Finkolo diorite dated at 2049 ± 38 Ma, (Liegeois et al., 1991) and massifs granitoids.

The Faleme volcanic belt is formed from West to East by the Saboussire formation and the Keniebandi formation.

The Saboussire formation a combination of volcanic and volcano-sedimentary

facies. This formation occupies the North-western half of the window (from Kedougou to Kenieba). In the southern part, it forms a band of several kilometres wide along the Faleme river. Throughout the formation, there is a clear predominance of volcanics, which decreases towards the eastern edge where sediments dominate Bassot (1966).

Three major shear zones have been noted in the Mali sector: Banifing, Sassandra and Siekerole. The Siekerole shear is located between the Yanfolila belt and the Siguiro basin. The Banifing shear located between the Morila volcanic belt and the Bougouni basin extends to the South through the Sassandra fault.

The North-east to South-west trending Faleme volcanic belt, intersected to the East by the regionally significant Senegalo-Malian fault, forms the boundary of a narrow post-Eburnian graben. There appears to have been significant displacement along the fault or one of its parallel aftershocks, as the terrain to the East of the Senegal-Malian shear consists of birimian basin sediments (known as Kofi series in Mali).

The lithostructural and geochronological work carried out in the Baoule Mossi domain and in the Kedougou-Kenieba inlier supports a polycyclic evolution of the Eburnian orogeny (Bard, 1974; Milési et al., 1986; Ledru et al., 1988; Bertrand et al., 1989; Feybesse et al., 1989; Boher et al., 1992).

In Guinea, the belts are formed by:

- a high-quality gneissic complex (Roques (1948) and here called Guinean Gneiss), including banded and local migmatitic orthogneiss, paragneiss, micaschist, base rocks (amphibolite, amphibolo-pyroxenite and pyroxene - garnet metabasite), quartzite, iron quartzite (with pyroxene and garnet) and sparse ultrabasite;

- a plutonic suite, composed mainly of tonalite, granodiorite and granite, which transforms into two major batholiths, the Macenta to the West and the Tounkarata to the East.

- volcanic-sedimentary successions, including metabasite iron formations, bands (BIF) and pelitic sediments, which form elongated narrow belts (Nimba and Simandou belts) discordant with the Guinean Gneiss (Roques, 1948); and

- small leucocratic biotite and granite plutons intersecting the Guinean Gneiss.

The Nimba Mountains series outcrops at the heart of a vast asymmetrical synclinorium oriented North-east to South-east. The North-western flank of this fold is locally very upright and inverted. The South-east flank dips at 30° C - 60° C and gives access to most of the lithotectonic pile composed of three (3) similar formations, separated by internal syn-D1 thrust planes, which are responsible for the doubling of the lithological stack. Most complete formation comprises, from bottom to top:

- grey and black silts, shales with intraformational conglomerates passing laterally and/or upwards pure quartzites of conglombratic levels; The facies contain lenticular intercalations of metabasites and carbonate intercalations (Ca or Mn);

- ribbon quartzites and ferruginous (BIF).

The Simandou series also outcrops at the heart of a north-south trending

synclinorium (Feybesse & Milési, 1994). The same lithologies are found but in variable proportions: the silt-shale-pure quartzite-amphibolite association may be absent or reduced to one of the last two components (by stratigraphic and/or tectonic beveling I). Finally, there is a possible transition from the volcano-sedimentary unit to carbonate arkosic sandstones. Here too, reconstructions of the lithotectonic pile reveal tectonic redoubling.

In Senegal, Bassot (1966, 1987) subdivided the western part of the Kedougou-Kenieba inlier into two supergroups arranged in elongated NNE-SSW bands: Mako and Diale-Dalema.

In 2002, in the eastern part of the Kedougou-Kenieba inlier, Hirdes and Davis completed the structuring of the Senegal side by highlighting the Faleme volcanic belt (Figure 1).

The Mako/Diale transition zone is represented by the interface between the Mako volcanic belt and the Diale basin. It is made up of greenstone from the Mako belt, mainly basic volcanics, intermediate to felsic volcanics composed of andesitic lavas and abundant volcanoclastites interbedded with metasediments and metavolcanosediments. Concordant and discordant plutonic masses are also found. This study focuses on the transition zone between belts and Diale paleoproterozoic basin in Senegal.

The stratigraphy of the Birimian formations has long been debated in the West African Craton (discussed in Vidal et al., 1996, 2009; Baratoux et al., 2011; Kock et al., 2011, Lambert-Smith et al., 2016) and seems to find consensus with Bassot. However, little is known about the transition zones between birimian belts and their associated basins.

Petrographic and structural informations needed to understand their litho-structural architectures is insufficient or non-existent or when it does exist it is not in phase with the new field data. The need to update this information justifies the timeliness of this study in this area.

It is important to note that, despite the paucity of scientific documentation in certain regions, the transition zones between belts and basins in the West African craton remain terrains recognised for their geological potential for the genesis and development of mineralization. These include the Bissa, Inata, Essakane and Mana deposits in Burkina Faso; the Loulo, Kodieran and Gounkoto deposits in Mali; the Bonikro, Agbaou and Tongon deposits in Côte d'Ivoire; and the Sabodala, Massawa, Sofia, Makabingui and Petowal deposits in Senegal.

3.2. Magmatic and Tectonic Context

Major pioneering work done on Kedougou-kenieba Inlier was carried out as part of useful substances prospecting missions by the Mines Directorate of French West Africa: United Nations Development Program (UNDP) in eastern Senegal (Tagini, 1959; Gravesteijn, 1962; Bassot, 1963).

Petrographic and structural work includes large number of drilled cores giving a fairly accurate idea of the geology of Paleoproterozoic terrains of Kedougou

inlier, which locally are heavily lateritic or depositional covered. A lithostratigraphic scale was proposed by *Mission Sénégal-Soviétique de recherches minières (1972-1973)* and *Bassot (1963, 1966)*.

Since *Bassot (1963, 1966)*, the formations of Kedougou-Kenieba inlier have been the subject of numerous studies (see exhaustive bibliography in *Pawlig et al., 2006; Debat et al., 1984; Ngom, 1985; Diallo, 1994; Ngom et al., 2007; Cissokho, 2010; Theveniaut et al., 2010; Gueye et al., 2007, 2008; Lawrence et al., 2013; Bassot 1987; Dioh et al., 2009; Gozo et al., 2015; Dabo et al., 2017; Labou, 2019; Labou et al., 2020*) and all of which defining that Paleoproterozoic terrains of Kedougou Inlier are represented by the Mako volcanoplutonic belt and Diale-Dalema basin intersected by different generations of granitoids (*Bassot, 1966; Mission Sénégal-Soviétique de recherches minières, 1970-1973; Debat et al., 1982; Debat et al., 1984; Ngom, 1985, 1995; Ndiaye, 1986, 1994; Dia, 1988; Dia et al., 1997; Diallo, 1983, 1994; Dioh, 1995; Dioh et al., 2006; Pawlig et al., 2006; Gueye et al., 2008; Hirdes & Davis, 2002; Delor et al., 2010*).

Bassot (1966, 1987) was the first to draw up a geological diagram of Kedougou-Kenieba inlier based on lithological and structural characteristics. In 1987, he subdivided this inlier into two supergroups arranged in elongated North North-east bands: Mako and Diale-Dalema. The western zone (Mako series) is oriented North North-east for 70° North-west (*Debat et al., 1984; Ngom, 1995*) and is intersected by the Badon batholith. Radiochronological data show that the Diale formations (sediments 2096 ± 8 to 2156 ± 10 (*Milési et al., 1986*); grauwackes 2165 ± 0.9 (*Hirdes & Davies, 2002*), are younger and based on the Mako volcanic formations (basalt ages between 2063 ± 41 and 2197 ± 13 Ma (*ABouchami et al. 1990; Dia, 1988*); andesite 2160 ± 16 Ma (*Boher, 1992*); rhyolite 2067 ± 12 Ma (*Gueye et al., 2007*)). More recent radiochronological data show the presence of metamorphic and magmatic rocks from the Mako belt dated between 2200 and 2070 Ma (*Gueye et al., 2008; Hirdes & Davis, 2002; Dia et al., 1997; Lambert-Smith et al., 2016*). Mako belt is the main source of detritus in the Diale-Dalema series. The dominant ages in the Diale-Dalema series range from 2200 to 2100 Ma (*Kone 2020*).

After *Bassot*, a lithostructural subdivision of Kedougou Kenieba Inlier with four series was proposed by *Gueye et al. (2007)* b, *Lambert-Smith et al. (2016)* on basis of *Bassot (1966)* and *Ledru et al. (1991)*. The boundary between Mako and Diale is defined by *Ledru et al. (1988)* at the Main Transcurrent Shear Zone (MTZ) while presence of detritical facies to the western side of this *Ledu et al. (1989)* boundary raises many questions about extension of sedimentary basin.

Later, *Sow (2004)* shows that the tectonic evolution of the Mako belt is characterised by three major shear zones such as the MTZ, the Yaakar Transcurrent Zone (YTZ) and the Sabodala Shear Zone (SSZ). The YTZ is a major structure defined at the contact between volcanic, volcano-sedimentary and sedimentary formations. Regionally, this structure appears to define a corridor of deformation with the MTZ where a mylonitic foliation is evident. The tectonites observed are strongly deformed in some places, and some show a line of stretching when plunging to the South or South South-east. This highlights a minor downthrusting of sedimentary

units onto volcanic and pyroclastic units across the steeply dipping YTZ.

Diene et al. (2012) define that the MTZ is discontinuous and associated to western and eastern branches with ponytail branches to the South.

Ganne et al. (2012) show that subduction lead to the burial of sediments at around 33 km during D1 compressive tectonic phase. This rock burial stage is followed by decompression of the associated units with a gradual increase in the thermal gradient from 15°C per Kilometer to around 50°C per kilometer during the second stage of transcurrent deformation (D2). This second phase is responsible for the amphibolite facies metamorphism at the contact with granitoid intrusions expressed by garnet, staurotide, chlorite, cordierite, plagioclase, kyanite, sillimanite, biotite, ilmenite, rutile and quartz assemblages.

The structural evolution of the Eburnian phase has been interpreted by various authors as being monocyclic (*Leube et al., 1990; Abouchami et al., 1990*) or polycyclic (*Feybesse et al., 1989; Ledru et al., 1991; Milesi et al., 1992; Ledru et al., 1988, 1991*) provide the following information: D1 is tangential and responsible for overlapping structures. It is dated at 2100 Ma (*Ledru et al., 1988*) and has been defined as an overlap (*Feybesse et al., 1989; Ledru et al., 1988, 1991; Milesi et al., 1992*) or a periplutonic deformation (*Pons et al., 1995; Vidal et al., 1996; Debat et al., 2003; Pitra et al., 2010; Delor et al., 2010*); D2 is transcurrent and associated with sinistral submeridian shears. It constitutes a transcurrent to transpressive deformation corridor responsible for Eburnian tectonics marked by major North-south to North-east structures and plutonic intrusions in Proterozoic terrains (*Ledru et al., 1988, 1991; Liégeois et al., 1991; Pons et al., 1995*); D2 is a sinistral transpression with North North-east to South South-west shortening (*Dabo et al., 2018*). The D3 phase is marked by dextral detachments (*Feybesse et al., 1989*).

Within the Kedougou inlier, a close spatial association between shear zones and Eburnian granitoids has been established (*Gueye et al., 2008*), showing a genetic link between magmatism and deformation (shear zones). Phase D1 is linked to crustal thickening (*Gueye & Ngom, 2020*). Whereas D2 tectonics leads to the folding of the first schistosity in the sedimentary ensemble of the Mako belt in the form of a vast North-east to South-west trending antiform, with an S2 schistosity as the axial plan (*Dabo et al., 2017*).

3.3. Geochemical Context

Geochemical studies of ultramafic rocks of Mako belt shows for most of auteurs of Mako (*Baratoux et al., 2011, Dia, 1988; Abouchami et al., 1990; Diallo, 1994; Dioh, 1995; Ngom, 1995; Diallo, 2001; Pawlig et al., 2006; Ngom et al., 2007; Ngom et al., 1998, 2010; Dabo et al., 2017; Ngom, 1995; Cissokho, 2010*); of Ghana (*Loh & Hirdes, 1999; Attoh et al., 2006; Dampare et al., 2019*), of Katiola-Marabadiassa en Côte d'Ivoire (*Pouclet et al., 2006*), of Bouroum Yalogo au Burkina Faso (*Ouedraogo, 1985*) and of Kadiolo au Mali (*Sangare, 2008*) that ultrabasites correspond to a single entity associated with undifferentiated tholeiitic series. Only the Loraboué ultrabasites (*Beziat et al., 2000*) are associated with calc-alkaline series described in the West African Craton.

For mafic rocks, some authors show the existence of two types of tholeiites (Zonou, 1987; Baratoux et al., 2011 in Burkina Faso; Ama Salah et al., 1996 in Niger and Pouclet et al., 1996 in Côte d'Ivoire) without specifying the geodynamic context, while others recognise only one type of tholeiite, either tholeiite1 or tholeiite2 (Dia, 1988; Abouchami et al., 1990; Diallo, 1994; Dioh, 1995; Ngom, 1995; Diallo, 2001; Pawlig et al., 2006; Ngom et al., 2007, 2010 in Mako; Sangaré, 2008 in Mali; Loh & Hirdes, 1999; Attoh et al., 2006; Dampare et al., 2008, 2009, 2019 in Ghana).

Labou et al., 2020 have recently identified three magmatic suites in the Mako belt from three different sources in both mafic and ultramafic rocks. In ultramafic rocks, the three types of association recognised are related to tholeiites 1, tholeiites 2 and calc-alkaline rocks.

3.4. Geodynamic Context

Geodynamic context of Mako calc-alkaline series is a volcanic arc (Bassot 1987; Dia, 1988; Boher et al., 1992; Diallo, 1994; Dioh, 1995; Moussolo, 2000; Diallo, 2001; Dioh et al., 2006; Theveniaut et al., 2010; Gozo et al., 2015; Gozo et al., 2015).

The geodynamic context of the tholeiitic series is the subject of controversy. Indeed, Bassot (1966) shows that the Mako Group formations were emplaced in an ocean floor environment;

Abouchami et al. (1990) maintain that Mako volcanism was emplaced in an environment comparable to oceanic shelf basalts without the influence of continental crust;

Ngom (1995), Ngom et al. (2007, 2010), Cissokho (2010) and Thievenaut et al. (2010) believe that Mako volcanism is comparable to N-MORBs or oceanic shelf basalts;

Dia (1988) and Dia et al. (1997) show that in the northern part of Mako, the tholeiitic volcanism has transitional geochemical characteristics between the N-MORBs and those of the IATs; this brings them closer to tholeiites of immature intra-oceanic arcs or presence of back-arc basalts;

Diallo (1994), Dioh (1995) and Diallo (2001) maintain that Mako tholeiitic series was placed in an oceanic island arc environment;

Pawlig et al. (2006) define that the rocks of the Mako Group are juvenile and derived from a depleted mantle source in an island arc environment;

Dabo et al. (2017) believe that the Mako mafic-ultramafic complex represents the lower unit of an ophiolite-like lithospheric fragment of the Birimian crust close to OIBs (Ocean island basaltes) or N-MORBs.

Recently, Labou et al. (2020) highlights two tholeiitic series from a separate source and argued that the tholeiitic1 series shows signatures comparable to MORBs, while the tholeiitic2 series and calc-alkaline series are compatibles with an arc environment.

4. Methodology

Methodology used to carry out this work is a mixed combinatory approach of quantitative and qualitative methods marked by a literature review and valuation of

available data, sampling and use of complementary data, geophysical, petrographic and geochemical study, modelling, analysis, interpretation and discussion. Two mapping campaigns and complementary data collection were carried out in collaboration with Randgold Resources (actual Barrick gold), who provided facilities and means of locomotion in the field. Samples were first collected: nineteen (19) outcrop samples and three hundred and seventy-nine (379) core samples drilling to update the geological map. For a better understanding of the study area, another field campaign was carried out with one hundred and nineteen (119) rock samples from outcrops and boreholes diamond drilling to complete updating of geology.

In addition, a total of fifteen (15) thin sections, nine (9) polished sections, twenty-four (24) Quemsan analyses and twenty-four (24) geochemical analyses were carried out for additional information.

4.1. Geological Mapping

Over entire study area, the practice consisted in carrying out a general survey of the outcrop (power, lifting the extension contour and noting the coordinates given by the Global Position System (GPS)). Outcrops were identified, described, and represented on the field minute. Structural data were recorded from measurements taken throughout the field campaigns. The measurements taken are mainly foliation directions and dips, schistosity planes, lineations, fold axes and, for brittle deformations, some fracture planes. The structural data were modelled using Stereonet. The interpreted structural maps were then digitized and processed with Arcview, Micromine and Géosoft. Geological mapping was used to produce interpreted lithological and structural maps. The lithostructural data were used to analyze tectonic structures.

4.2. Geophysical Mapping

Aeromagnetic surveys involve measuring the Earth's magnetic field in order to detect local variations due to magnetism. These anomalies reveal the geological structures of the Earth's crust, particularly the spatial geometry of rocks and the presence of lineaments interpreted as geological discontinuities (faults). Minerals such as magnetite (Fe_3O_4), ilmenite and pyrrhotite are generally present in endogenous rocks, particularly basic to ultrabasic rocks. They are considered ferromagnetic and are responsible for the magnetic susceptibility of rocks, which can be surveyed on the ground or remotely using a magnetometer (**Figure 2**).

Spectral radiometry or gamma spectrometry is another method of airborne prospecting. It is about recording the gamma radiation emanating from the first few centimeters of the ground. The radiometry is not the propose of this study, it is integrated and combined to fact-mapped data to redéfine geometric and geological characteristics of large plutonic masses. It highlights the ground levels of 3 elements: potassium (K), thorium (Th) and uranium (**Figure 3**). Each of these elements characterises a specific type of facies; for example, potassium abundance indicates the presence of an acidic facies such as granite.

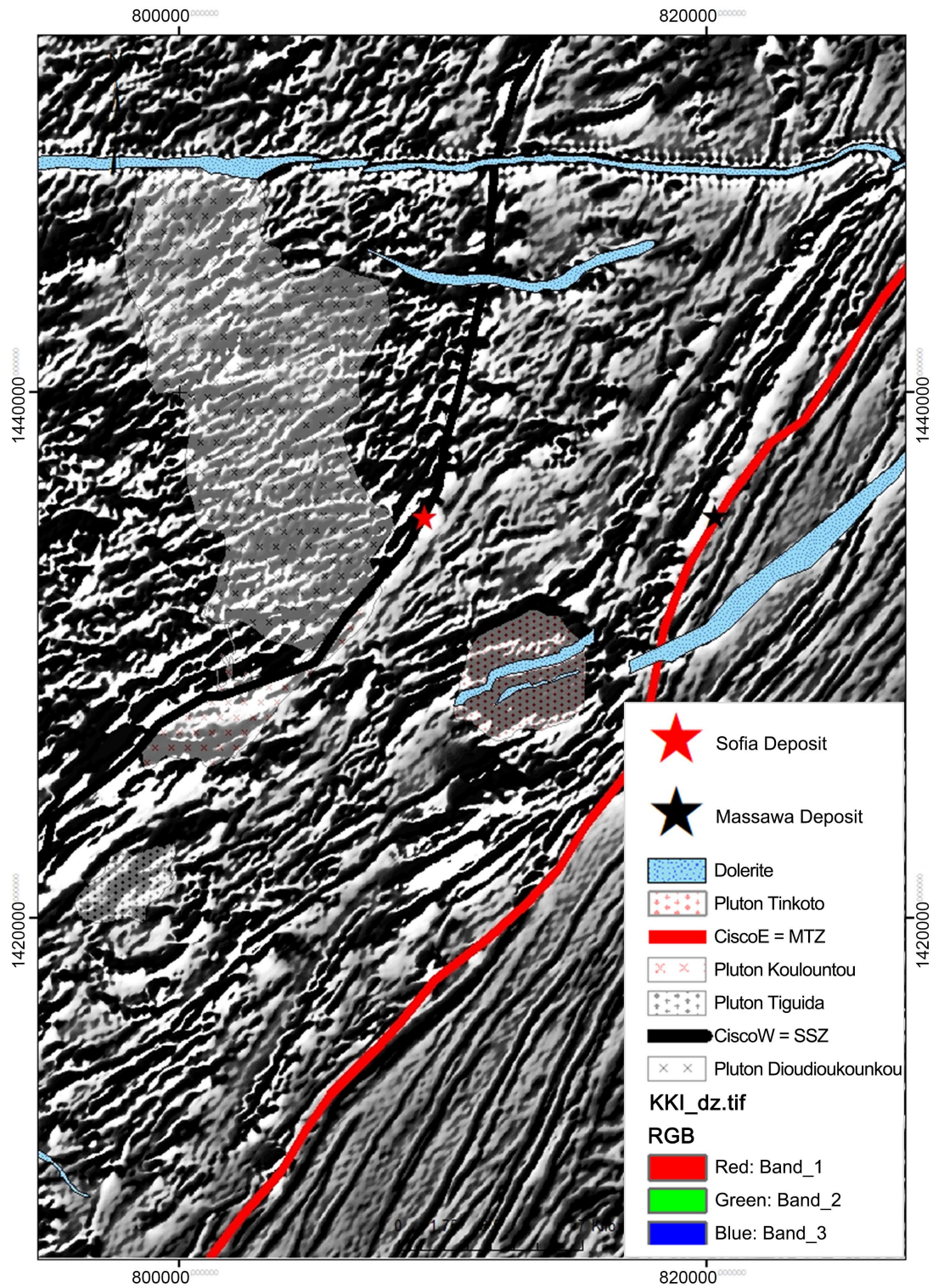


Figure 2. Total magnetic intensity map (grey-scale 1DV-division-) showing major. Magnetic intensity map highlights three zones with distinct magnetic signatures: a zone of high magnetic intensity to the West, with a fluidal texture; an intermediate zone of medium-to-high magnetic intensity, with a deformed, anastomosing semi-linear texture; and a zone of low to medium intensity, with a linear texture. These zones are bounded by two major shears: the Western Contact Shear Zone (CiscoW = SSZ called Sabodala Shear zone) and the Eastern Contact Shear Zone (CiscoE = MTZ named Main Transcurrent shear Zone).

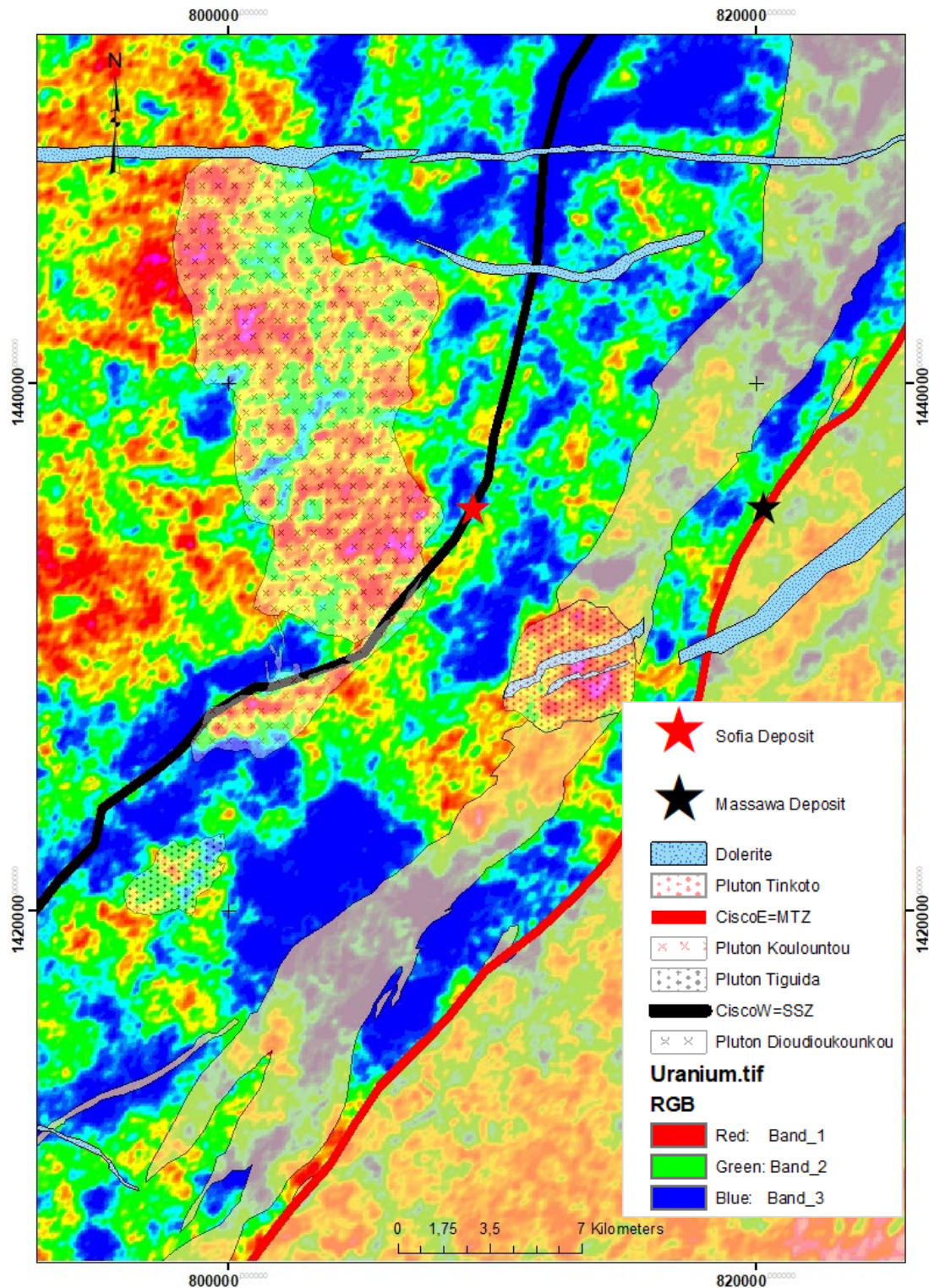


Figure 3. Radiometric map of variations in the spatial distribution of the Uranium concentration gradient. The Uranium distribution map shows the well-defined contours of the plutonic masses in the study area. Uranium concentration in the Dioudiokoukou pluton is highly heterogeneous, reflecting the diversity of facies found within the pluton. The highest Uranium contents are found in the South-eastern and North-western parts of the pluton Dioudiokoukou and Tinkoto.

4.3. Geochemical Analysis

Geochemical analyses were carried out using X-ray fluorescence spectrometry or XRF at the University of Lausanne. Twenty-four (24) samples were analyzed, providing in-depth scientific data on the study area. The samples included 2 gabbros, 2 diorites, 3 basalts, 5 andesitic facies, 3 volcanoclastites, 3 granodiorites, 2 granites, 2 volcanosediments and 2 sediments. Five (5) samples belong to diamond drilling holes, the nineteen (19) other samples from field outcrops.

Major element contents of the total rock (SiO_2 , TiO_2 , Al_2O_3 , Fe_2O_3 , MnO , MgO , CaO , Na_2O , K_2O , Cr_2O_3 and NiO) were determined on fused disks prepared from 1.2 g of calcined sample powder mixed with lithium-tetraborate (1:5 mixture). XRF calibrations are based on 21 international reference of silica rock. Data are reported on loss of ignition (LI) basis (**Table 2**).

Trace element analyses (Sc, V, Cr, Mn, Co, Ni, Cu, Zn, Ga, Ge, As, Se, Br, Rb, Sr, Y, Zr, Nb, Mo, Ag, Cd, Sn, Sb, Te, I, Cs, Ba, La, Ce, Nd, Sm, Yb, Hf, Ta, W, Hg, Tl, Pb, Bi, Th, U) were carried out on disks obtained by pressing 12 g of sample powder onto a Hoechst-wax-C support. Trace element calibrations are based on synthetic standards and international silicate rock reference materials. Detection limits depend on the element concerned, but are in the order of 1 to 7 ppm for trace elements and 20 to 80 ppm for major elements. Geochemical data were processed using GeoChemical Data ToolKIT.

4.4. Mineral Analysis

Quantitative Evaluation of Minerals by Scanning electron microscope (QUEMSCAN) were carried out at the Mineral resources and geofluids laboratory of the Department of Earth and Environmental Sciences at the University of Geneva. Thin and polished sections made in Ivory Coast at Felix Houphouet Boigny University were used as base samples. QUEMSCAN analysis is mineralogical and petrographic data acquisition system developed by the FEI company (a subsidiary of Thermo Fisher Scientific).

5. Results

5.1. New Lithostructural Architecture of the Mako-Diale Transition Zone

The lithostructural architecture established on the basis of new geological data (**Figures 2-4**) highlights three major structures: Western shear-contact (CiscoW), Median shear-contact (CiscoM) and the Eastern shear-contact (CiscoE). The CiscoW, CiscoM and CiscoE delineate three major lithostructural domains corresponding to Maco domain, Sesam domain and Diabba domain (**Figure 5**).

The Western shear-contact (CiscoW) is a North-south to North-east shear located between pillow lavas and andesitic to metavolcanic facies in the western part of area of study (**Figure 5**). The CiscoW forms the boundary between the Maco and Sesam domains. It corresponds to Sabodala Sinistral Mylonitic Shear Zone (SSZ).

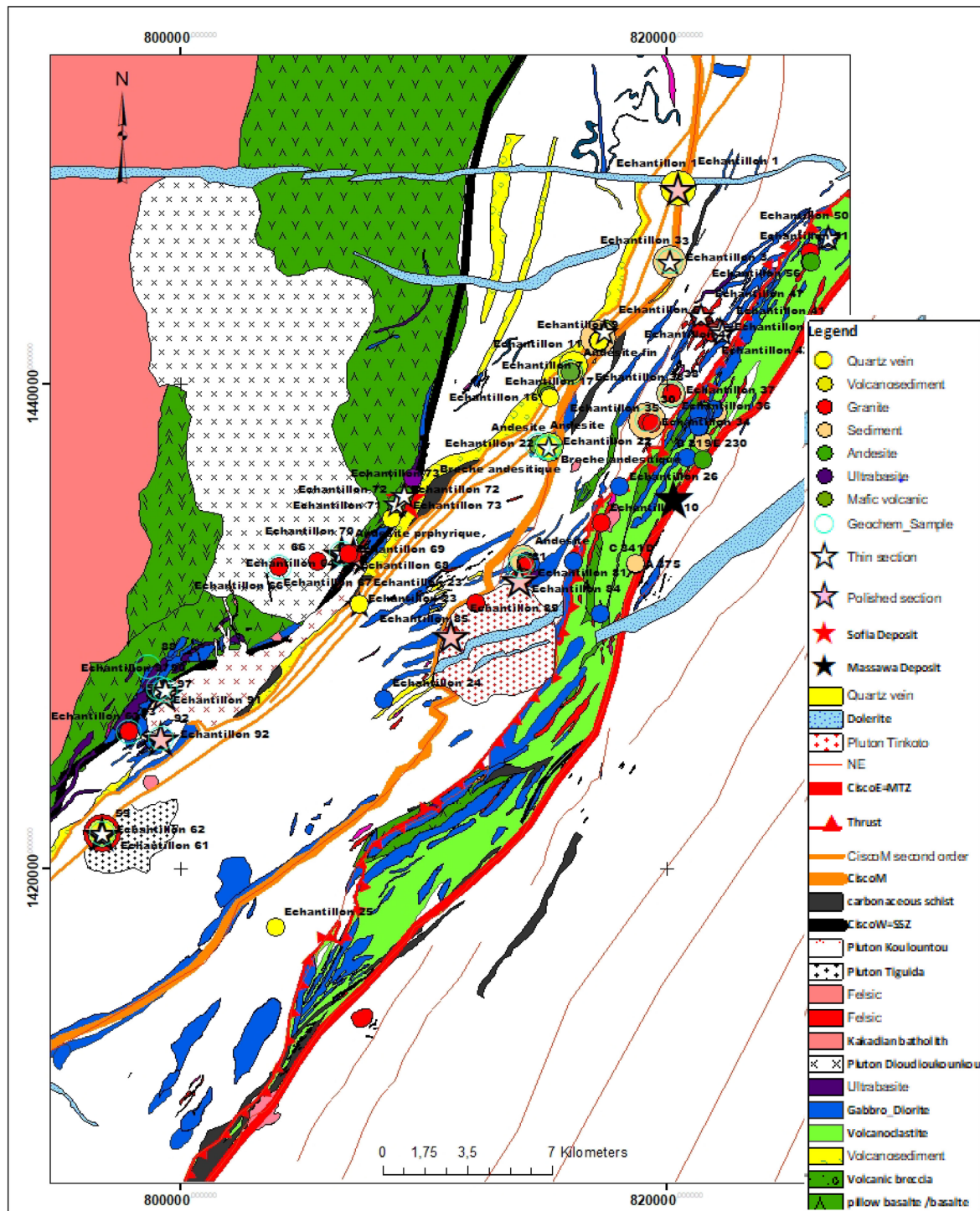


Figure 4. Location of samples collected and analyzed as part of this study. The samples (echantillons) shown in this figure come mainly from field mapping data. It should be noted that there are locally great overlapping due to selective sampling or to the proximity of certain points or again to the diversity of analysis carried out on some same samples. A more detailed and selective cartographic and petrographic studies of the zone with deformed semi-linear texture (see **Figure 2**: total magnetic intensity map) was carried out. This led to the definition of a median shear-contact (CiscoM) located between CiscoW and CiscoE and setting with two branches: the northern branch to the North of the study area is oriented N010 to N180 and dipping 56° C to 85° C. The North-east branch located to the South is trending N044 to N080 and dipping between 63° C and 90° C.

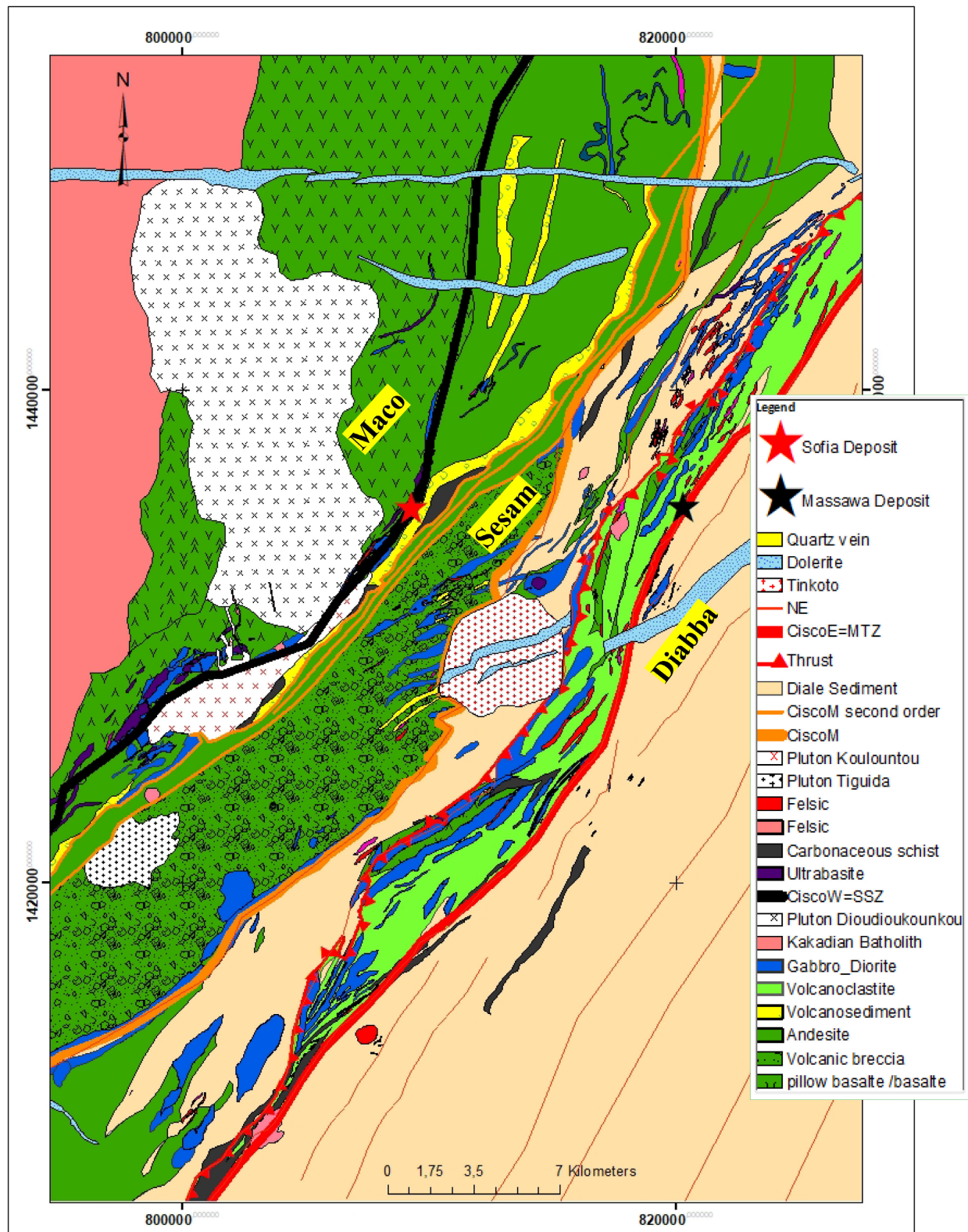


Figure 5. Lithostructural map of Mako-Diale transition zone. Maco domain located to the West of the western Shear-contact occidental (CiscoW); Sesam domain limited to the West by CiscoW and to the East by median Shear-contact (CiscoM); Diabba domain, located to the East of median Shear-contact (CiscoM). Volcanosediments in this map represent andesitic (explosive volcanic) deposited materiel with facies ranging from coarse to fine (ash) lithic elements¹.

The Median shear-contact (CiscoM) set as sinistral shear made up of two ranges of structures. A main branch that marks the lithostructural contact between Diabba and Sesam domains followed by second order structures. Main CiscoM sets with two branches: the northern branch located to the North of the area of study is oriented North-south. The main CiscoM southern branch is located to the South of the area of study and oriented North-east.

Eastern shear-contact (CiscoE) is a NE-trending dextral strike-slip, mainly regional in extent. It forms the eastern boundary of the Diabba volcanic formation located to the eastern part of the study area. The CiscoE correspond to Main Transcurrent shear zone (MTZ).

Maco lithostructural domain is located to the West of the Sesam domain. It is bounded to the West by the Mauritanides and to the East by the CiscoW. Lithologies are represented by metabasalts, ultrabasic, basic, intermediate and acid plutons.

Sesam lithostructural domain is located to the West of the CiscoM and Diabba domain. It is characterised by the presence of a volcanics associated with metavolcanodetritic sequences. Volcanics forms andesitic rock flows alternating with metamorphosed volcanosediments facies.

Diabba lithostructural domain located to the East of CiscoM. It is essentially made up of slightly metamorphosed sedimentary unit associated with volcanic belt. Volcanic belt is formed by a band of volcanoclastites and andesitic sequences that can be observed locally to the north, south and centre of the Diabba domain. Domains are intersected by plutonic complex.

5.2. Typologie of Major Tectonic Limites

5.2.1. The Western Shear-Contact (CISCOW)

The western shear-contact corresponding to Sabodala Shear (SSZ) is North-south to North-east trending fault located between the pillow lavas and the andesitic and metavolcanodetritic facies in the western part of the study area. It forms the limit between Maco and Sesam domains. The CiscoW takes the form of mylonitic shear zone (**Figure 6, Figure 7**). In the proximal parts of the CiscoW, the facies are very mylonitised and fine with minerals oriented along the deformation and located on either side of the shear zone. The CiscoW is associated with compressive deformation affecting, in addition to the Koulountou massif, facies representative of the mafic magmatic phase that led to the emplacement of ultrabasic and basic facies affected by folding (**Figure 8**). The

¹HIGH IMPORTANT MESSAGE: Carefully and close look at **Figure 5**

Maco is not a locality. Maco is not Mako, which means the volcanic belt (including Diale basin) within Kedougou Inlier

Maco represents the upper and western part of Mako bounded to the East by the CiscoW shear zone which is the equivalent of the Sabodala shear zone (SSZ).

Maco, Sesam and Diabba are not representing localities. They stand as names of three lithostructural domains that form, like puzzles of one-piece, the latest lithostructural architecture of the Mako-Diale transition zone. These are new terms introduced by the main author to designate the following acronyms:

MACO: Mako Croute Oceanique = Mako Oceanic Crust;

SESAM: Sequences et Series Andesitiques de Mako = Andesitic Sequences and series of Mako;

DIABBA: Diale Back-Arc-Basin = Diale Bassin arriere-arc.

CiscoW shows two directions, North-south branch to the North and North-east branch to the South.

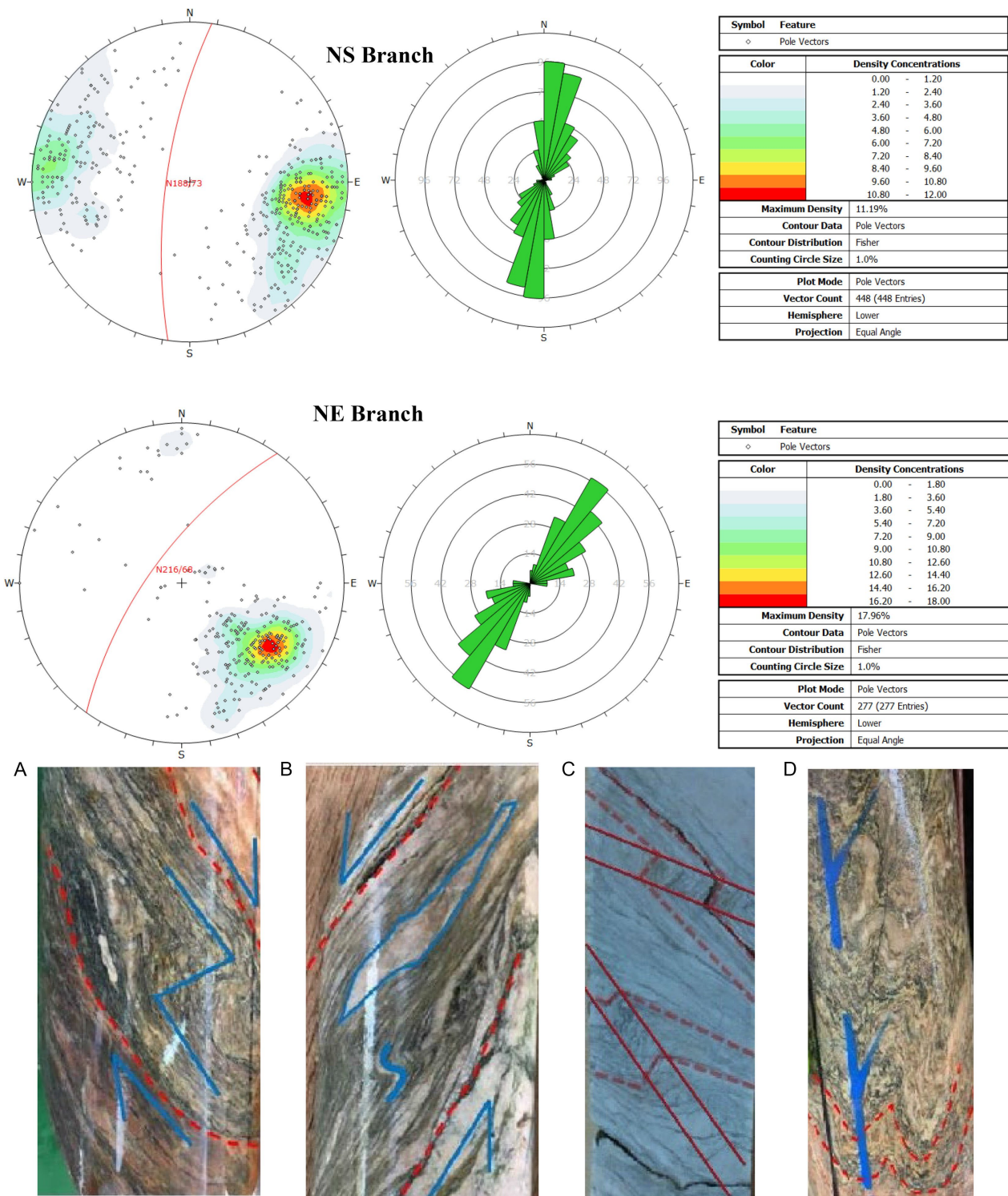


Figure 6. Structural characteristics of CiscoW shear zones and kinematic indicators of ductile deformation A: Z-fold showing reverse movement and boudinated/folded quartz veins; B: S-fold showing reverse movement of folded quartz veins and sigma clast pressure shadows; C: conjugated kink bands; D: W-fold hinge marker in a highly deformed zone.

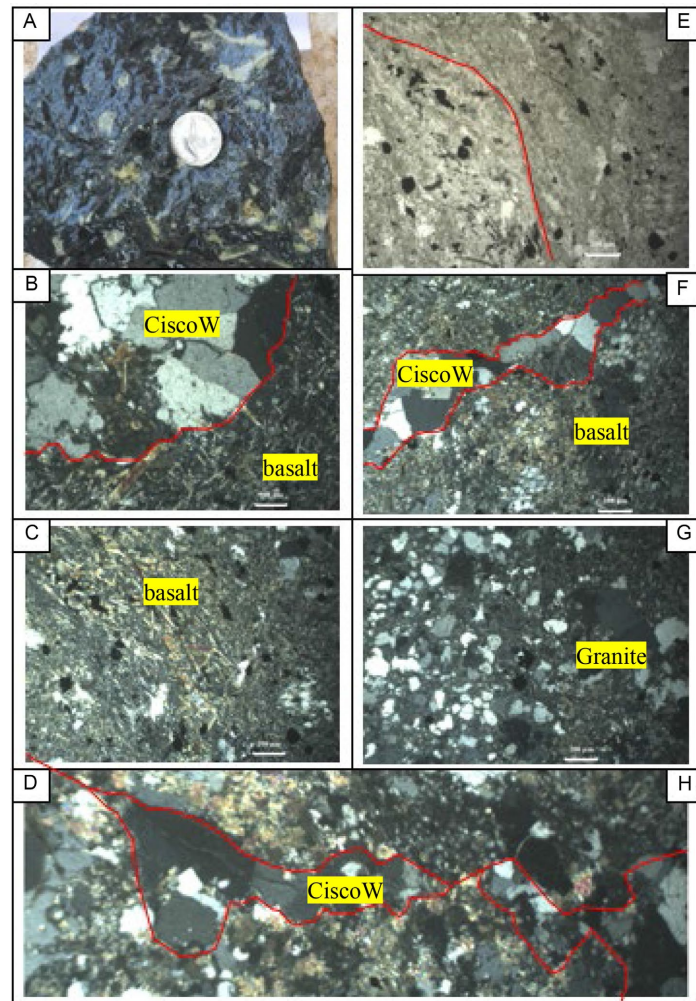


Figure 7. Western shear-contact (CiscoW) visible as a thin layer. The petrographic study highlights contact structure between the Kou-lountou massif and basaltic facies of the Maco. A: Rock sample at the contact of Koulountou granite and Maco); E: Natural light microphotography; B, C, D, F, G, H: Polarised light microphotography.

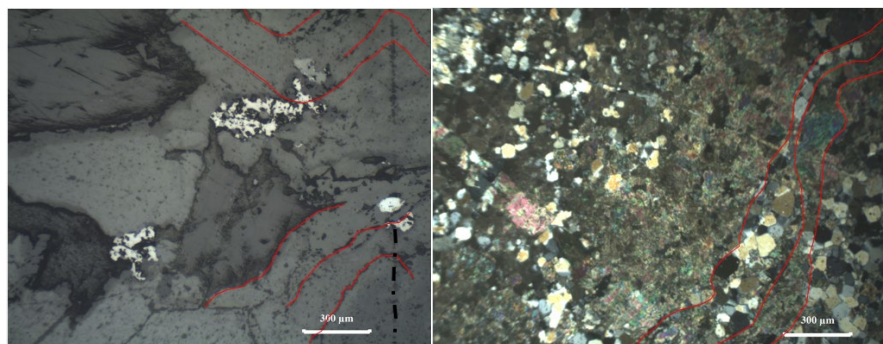


Figure 8. Polished sections on the Koulountou (sample 92) granodiorite showing folding and fold hinges to the south of the Koulountou massif; Microscopic analysis also shows the presence of folding indicators, in particular the hinge zones of anticlines and synclines, evidence of ductile deformation tectonics visible on the microphotographs of the Kou-lountou massif along the CiscoW.

5.2.2. Median Shear-Contact (CiscoM)

The CiscoM runs sub-parallel to the Western shear-contact (CiscoW = SSZ). The CiscoM (**Figure 9**) is a ductile then brittle shear zone with a schistosity showing two main directions North-south and North-east with fairly steep dips. It consists of a main structure associated with three other second-order structures. The main structure has two branches: the main branch to the North of the area of study is oriented N010 to N0180 and dips 56° C to 85° C. The North-eastern branch is located to the South, trending N044 to N080 and dipping between 63° C and 90° C.



Figure 9. CiscoM outcropping with boudinated quartz veins at the contact between sheared and baked fine sediment (schistes) and andesitic sequence of Sesam.

5.2.3. Eastern Shear-Contact (CiscoE)

The CiscoE corresponds to the Main Transcurrent Shear zone (MTZ). It stands as shear-contact that marks the eastern limit of the volcanoclastites associated with Diabba domain. The CiscoE is regional in extent, running North-east to locally North-south. It consists of a main branch that is continuous throughout the area of study and sub-parallel and discontinuous second-order structures. The CiscoE forms the eastern limit of the Diabba volcanic formation located to the east of the study area. It forms a brittle-ductile shear zone with an average thickness of 0.3 meters (**Figure 10**). Its length covers the entire study area. It marks the eastern contact between the volcanic and sedimentary formations of Diabba in this area of study. CiscoE is marked by a brittle-ductile deformation and intense graphite or else by breccia or regional brittle deformation.

5.3. Petrography/Mineralogy of Main Domains Formations

5.3.1. Maco Formations

They are mainly represented by massive or pillowed (**Figure 11A**, **Figure 11B**) metabasalts and ultrabasic, basic, intermediate and acidic plutonic formations such as ultrabasites, gabbros, diorites, granodiorites and granites.

Dacites are greyish-green effusive rocks rich in quartz and plagioclase. They are

weakly porphyritic lavas with plagioclase phenocrysts and microphenocrysts. Calcite and quartz veinlets are present (**Figure 11A**).

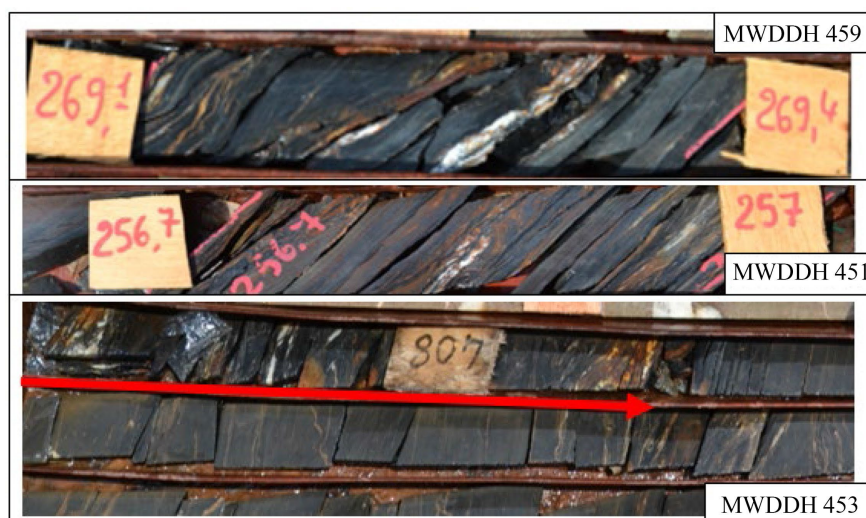


Figure 10. Extension of the CiscoE main shear zone.



Figure 11. Basaltic facies of Maco. A: massive basalt; B: Pillow basalt.

5.3.2. Sesam Formations

Sesam is mainly represented by andesitic volcanic formations (breccias, meta-andesite, metavolcanosediments, metatufs) associated with andesitic volcanosediments. A complex of plutonic ultrabasic, basic et acid and mafic to felsic volcanics are associated to Sesam formations. Explosive andesitic volcanism formed by accumulations of projections in massive or porphyritic form, or breccias. Andesitic flows alternate with agglomerates, tuffs and abundant volcanic breccia (**Figure 12**).

5.3.3. Diabba Formations

Diabba main lithologies are composed of sedimentary facies (fine-grained sediments, schists, quartz veins, cherts, metapelites, conglomerates, grauwackes (**Figure 13**, **Figure 14**) associated with metabasalts, volcanoclastites, metarhyodacites. Diabba formations are affected by a series of structures marked by large-scale folding associated with ductile and brittle shearing. The ductile structures form major shear zones and local sub-parallel thrusting North-east trending. Brittle structures accompanying folding and shearing are represented by fractures and reverse faults.

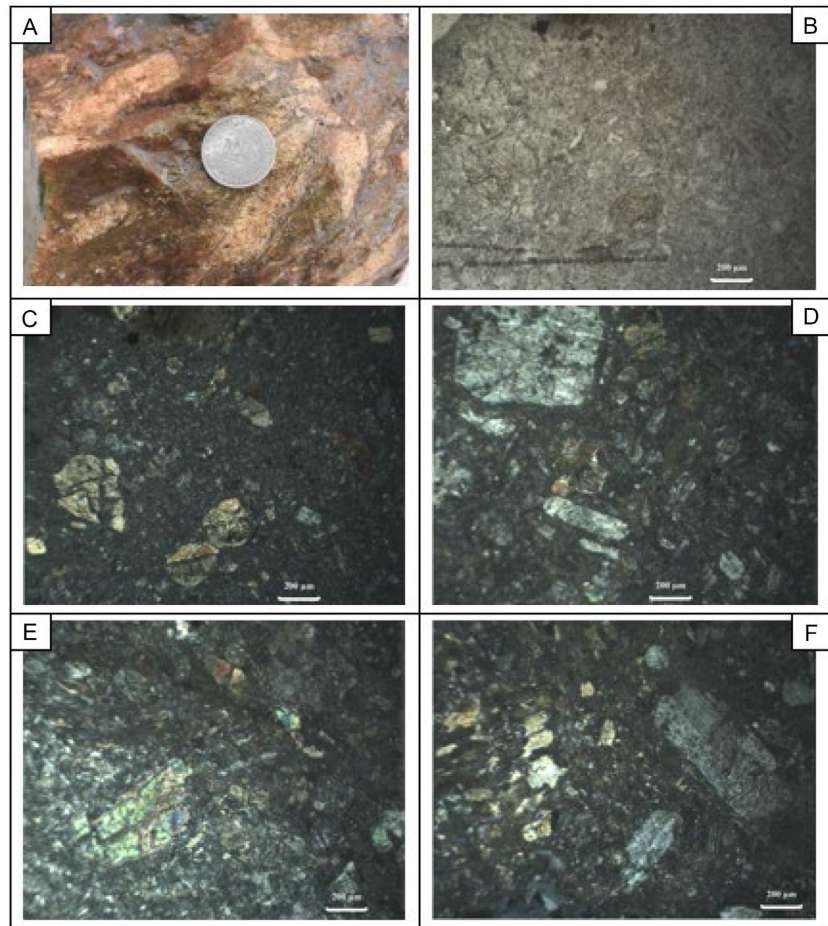


Figure 12. Sesam polygenic breccia. A: Rock sample from outcrop (polygenic breccia); B: Natural light microphotography; C, D, E, F: Polarised light microphotography. The breccias and volcanic agglomerates (A, B, C, D, E, F) are associated with light-green tuffaceous material mainly oriented N025 with a dip of 60° North-west. The facies is deformed by schistosity marked by the stretching of millimeter to centimeter clasts arranged parallel to the direction of the tuffites.

5.4. Typologie of Large Plutonic Masses

5.4.1. The Dioudiokoukou Pluton

Dioudiokoukou is a circumscribed North-south trending massive intrusive of almost oval shape with irregular rims covering an area of about 60 km². The Dioudiokoukou granite is composed of automorphous to subautomorphous plagioclase with saussauritic core. Quartz is moderately abundant in small interstitial patches. Chlorite (3% to 3.6%) and green hornblende (1.3% to 1.7%) are widespread. Dioudiokoukou contains two facies (coarse primary facies and finer secondary facies). The primary facies surround the secondary along a quartz vein. Dioudiokoukou contain two enclaves types: basaltic and andesitic. Basaltic enclaves are content relics of slightly deformed minerals (pyroxenes, plagioclases and amphiboles). Andesitic enclaves show plagioclases that have been badly affected by ductile and then brittle shearing after a phase of ductile deformation (folding).

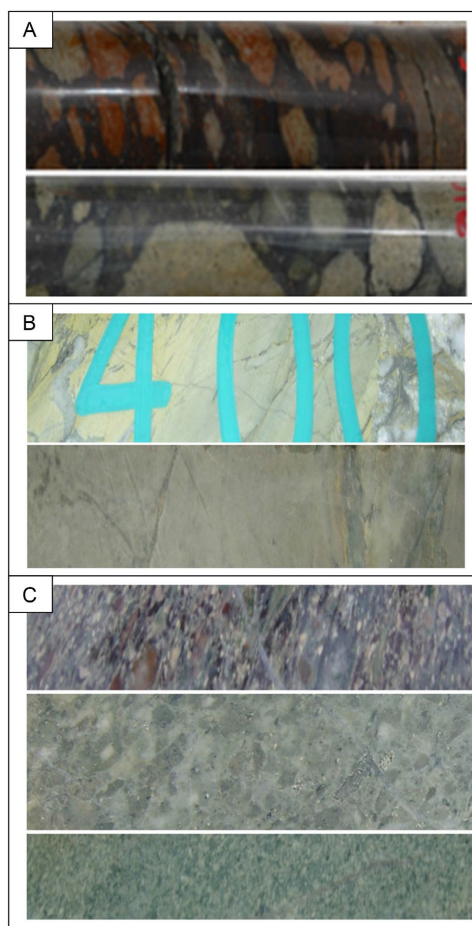


Figure 13. Volcaniclastic facies within Diabba domain. A: Facies with coarse clasts; B: Vitreous facies; C: Facies with medium to fine grains. Facies with large lithic elements or lapilli tuffs are formed of large sub-angular to stretched polygenic clasts several tens of millimetres long with a rare, ashy cement (A). They are rich in rock fragments and quartz grains. These facies are often associated with highly sheared to brecciated graphitic contacts. These rock are also affected by intense silicification. Facies with medium to fine sub-rounded to sub-stretched clasts, 64 millimetres in size, of varied nature, are andesitic with a predominance of mauve or green clasts (C). The cement is tuffaceous, not very abundant and of the same nature as the dominant clasts. The vitreous facies or volcaniclastic ash (B), which is a vitreous matrix with no visible clasts. The kinerites show a strong network of alterations and quartz veins. Microscopic study shows that the volcanoclastite varieties correspond to: Volcanoclastic metallitharenites composed of volcanic lithoclasts, hornblende, plagioclase clasts and quartz united by a rare matrix (almost contiguous grains) that is finely recrystallised; Volcanoclastic quartzofeldspathic meta-arenites with polygenic lithoclasts corresponding to rock formed from lithoclasts, plagioclases and quartz united by an intensely calcitic quartzofeldspathic cement. The abundance of microlitic porphyritic andesitic lithoclasts may also justify a name; Feldspathic volcaniclastic meta-arenites with rare clasts constitute locally microlithic rock made up of mineral fragments and rock in a relatively abundant recrystallised cement. Lithoclasts are rare and very small, and the rock is highly deformed with competent brecciated beds. Schistosity is marked and the rock is intensely invaded by fluid circulation; Volcaniclastic meta-lutites composed of ferromagnesian, quartz clasts and plagioclases bound together by abundant cement. The rock is altered to chlorite, sericite and calcite, with quartz clasts and plagioclases bound together by abundant cement.

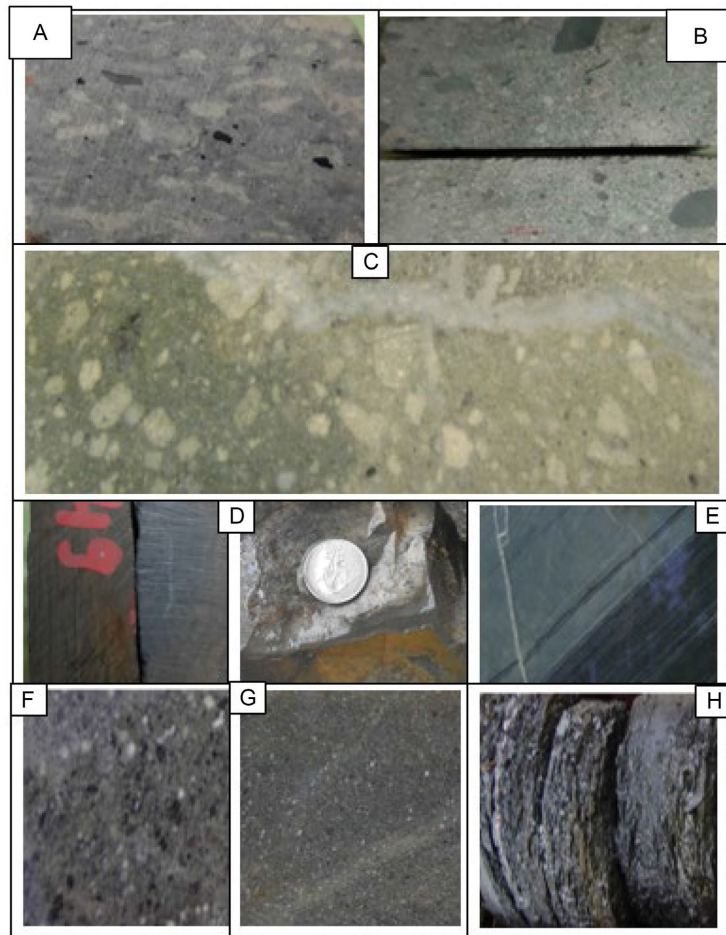


Figure 14. Several examples of metasedimentary facies of Diabba domain. A, B: Northern conglomerates; C: Southern conglomerates; D, E: Fine to pelitic sediment; F: Coarse-grained grauwacke; G: Medium to fine-grained grauwacke; H: Carbonaceous shales. The conglomerates are practically made up of epiclasts of sedimentary nature with sparse cement of a fine pelitic nature (A, B, C). The facies is discontinuous and the elements are polygenic in blunt to subrounded form, indicating transport between their source and their depositional environment. The very coarse-grained greywackes (F) contain relatively coarse clasts in a sparse to abundant matrix. Apart from the grain size, this facies can have all the characteristics of fine and medium grauwacke. This facies is dominant in the northern part of the prospect and is often interspersed with levels that are sometimes very graphitic and highly deformed, forming the wall of mineralisation. The medium-grained greywackes (G) show well-individualised grains or small clasts in mostly chloritised and sericitised matrix and the rock is generally criss-crossed by a system of quartz, carbonate or hematite veins and veinlets. The graphitic metapelites (D, E) are characterised by a bedding with alternating coarser light beds and fine graphitic beds. Sericite levels and quartz and carbonate veins are associated with this bedding oriented N020 with dip of 70° to 85° and which can be taken up by shearing. Graphitic shales (H): when the graphitic facies are sheared and affected by intense deformation, they are very shaly and strongly graphitised; they thus become graphitic shales and shear zone. They may constitute small edge passage or form a large package. Graphitic schists are common in fine sediments and fine volcanoclastites. They may be intersected at contact between volcanoclastites and intrusives.

5.4.2. The Tinkoto Pluton

Tinkoto is a rounded to locally subrounded massif. Tinkoto granite outcrops sets

in the form of metric-sized balls. It is found in bed of rivers, valleys and within lateritic armour. The texture is most often grainy with light whitish-pink colour reflecting the presence of alkaline feldspars and quartz. It is an unconformable granite. Outcrops occur in the form of scattered blocks rarely exceeding ten metres in diameter. It has coarse to medium-grained texture with an uneven distribution of K-feldspar phenocrysts. Melanocratic enclaves can also be found in the massif. Tinkoto massif also shows veins complex set in fracture network. The veins strike mainly N055 and N010. Facies could locally be grey isogranular, with automorphic quartz (irregular edge) showing undulatory extinction and greyish patches forming. Subautomorphic plagioclases show polysynthetic macles or clear double macles. Other facies show heterogranular micrograined texture. Clear sections often include green hornblende or biotite. Crystals may show quartz recrystallisation on edges. Plagioclase crystals are automorphous and sometimes grouped in polycrystalline clusters. Biotite occurs as automorphous sheets, locally embedded in plagioclase.

5.4.3. The Koulountou Pluton

Koulountou pluton (**Figure 15, Figure 16**) is an elliptical massif, narrowed and stretched in its northern part in a North-east direction. It takes the form of blocks that can be several metres in diameter. They are mainly located in the South of Sofia deposit and composed of plagioclase, amphibole, and quartz. They are strongly altered in carbonate-quartz, sericite and pyrite. The main types of alteration are chlorite, sericite, carbonate, limonite and leucoxene. The rocks are also crossed by aplites in places. Deformation is visible in minerals and is made up of fractures. The walls of these fractures are lined with chlorite in places. Note that the late veins are more acidic, with pinkish tinge tending towards a granitic composition. The minerals vary in size, becoming larger to the South. They are only slightly deformed and are made up of fractures. The walls of the fractures are lined with chlorite in places. The late veins are more acidic, with pinkish tinge tending towards a granitic composition.

5.4.4. The Tiguida Pluton

Tiguida pluton (**Figure 17**) outcrops to the South of the Koulountou massif over several kilometres along strike N032 in an elliptical shape. It is facies rich in potassic feldspar. Mineral composition shows plagioclase-Ab-Ol (54.11%), Quartz (29.49%), Illite (5.60%), Muscovite (4.89%), Calcite (2.24%), Chlorite (1.86%), garnet granite (andradite). It shows large fracture network mainly oriented N050/80 with surface alteration revealing relics of acicular and coarse grains quartz.

5.5. Geochemical Signatures

5.5.1. Geochemical Signature of Maco

The study (majors and traces) of the formations of Maco domain lithostructural (**Table 1**) highlights two groups of magmatic rocks: calc-alkaline volcanic rock and sub-alkaline to tholeiitic rocks, which are plutonic formations.

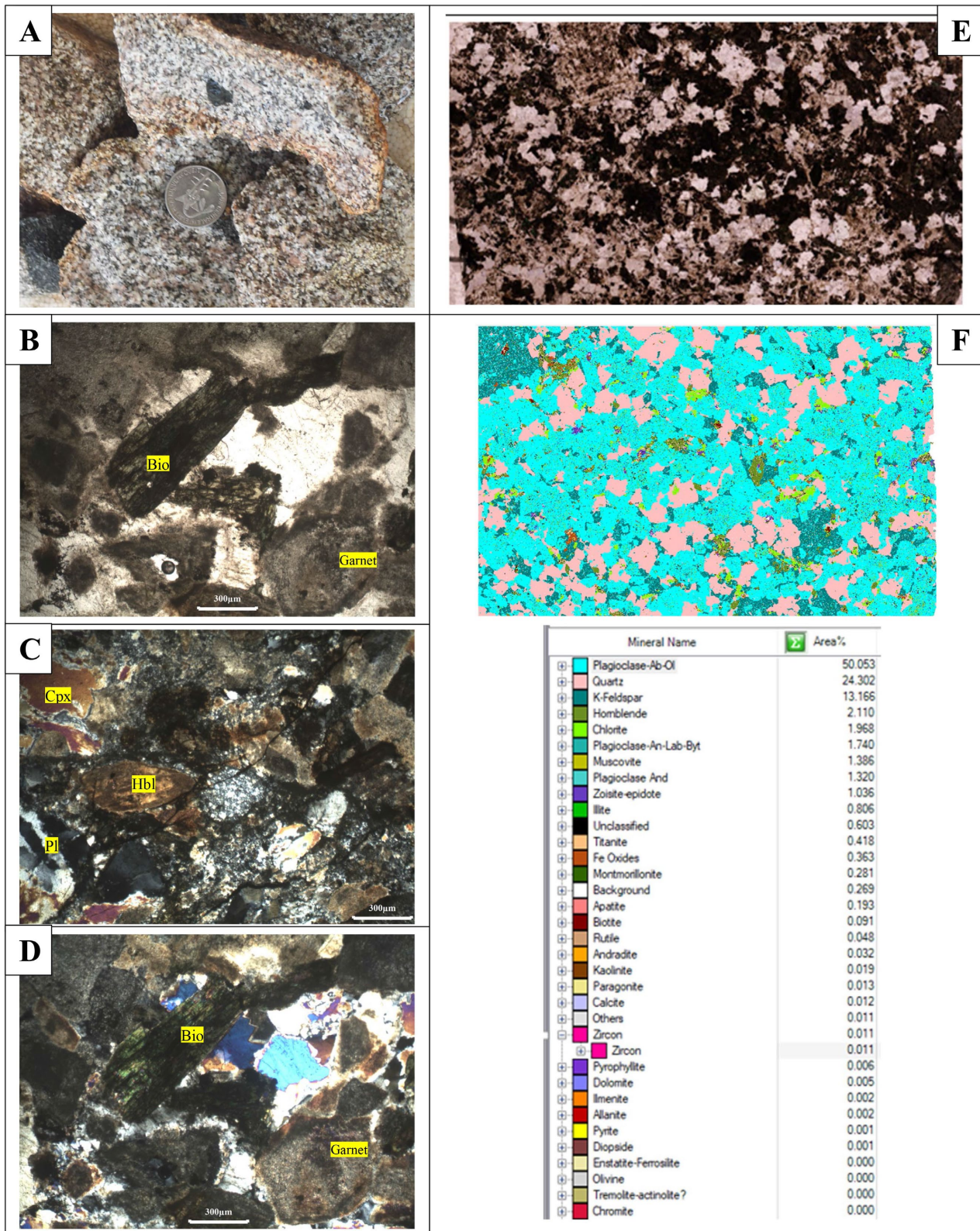


Figure 15. Facies of the Koulountou pluton. A: detail of Koulountou granite outcrop; B, C, D, E: detail of microphotographs of Sample 100 in polished section; F: QEMSCAN analysis giving mineral composition of sample 100: plagioclases (50.05%), Quartz (24.30%), K feldspar (13.16%), hornblende (2.11%), Chlorite (1.96%).

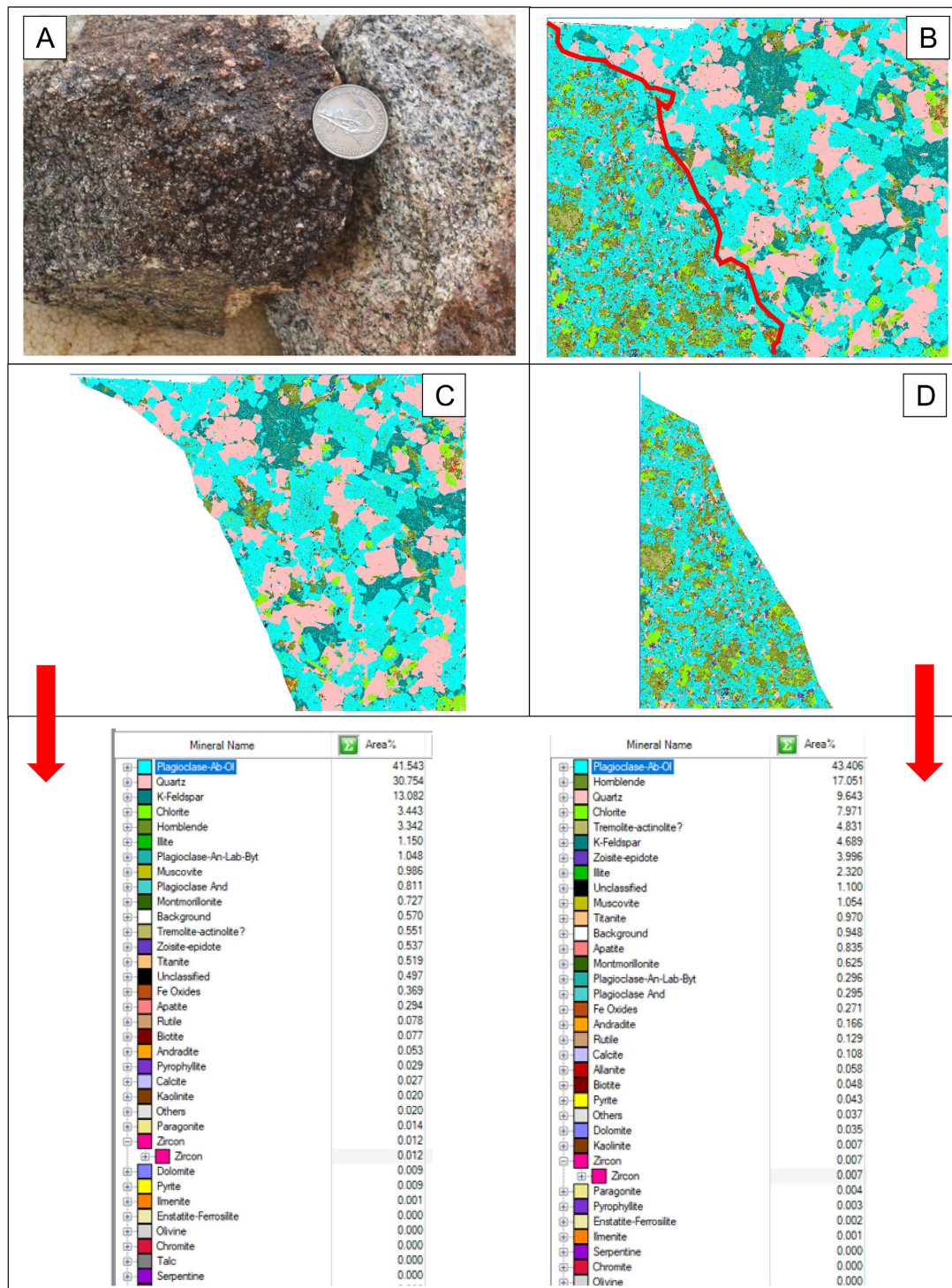


Figure 16. Other facies of Koulountou Pluton. A: representative facies (sample97) of Koulountou granite in polished section analyzed by Quemscan in contact with Maco basalt; B: Maco basalt (sample 97): plagioclase (43.406%), hornblende (17.05%), quartz (9.64%), chlorite (7.97%), K feldspar (4.68%); A: Koulountou granite (sample 97): plagioclase-Ab-Ol (41.543%), Quartz (30.75%), K feldspar (13.08%), hornblende (3.34%). The sample 97 shows plagioclases, amphiboles and quartz Orthose is common with the Carlsbad mark well individualised. Ferromagnesian minerals such as biotite and amphibole are visible in the altered parts. Koulountou contains enclaves that are essentially ultrabasic and basaltic. They are millimetre to centimetre in size (up to one decimetre). They are strongly altered in carbonate-quartz, sericite and pyrite.

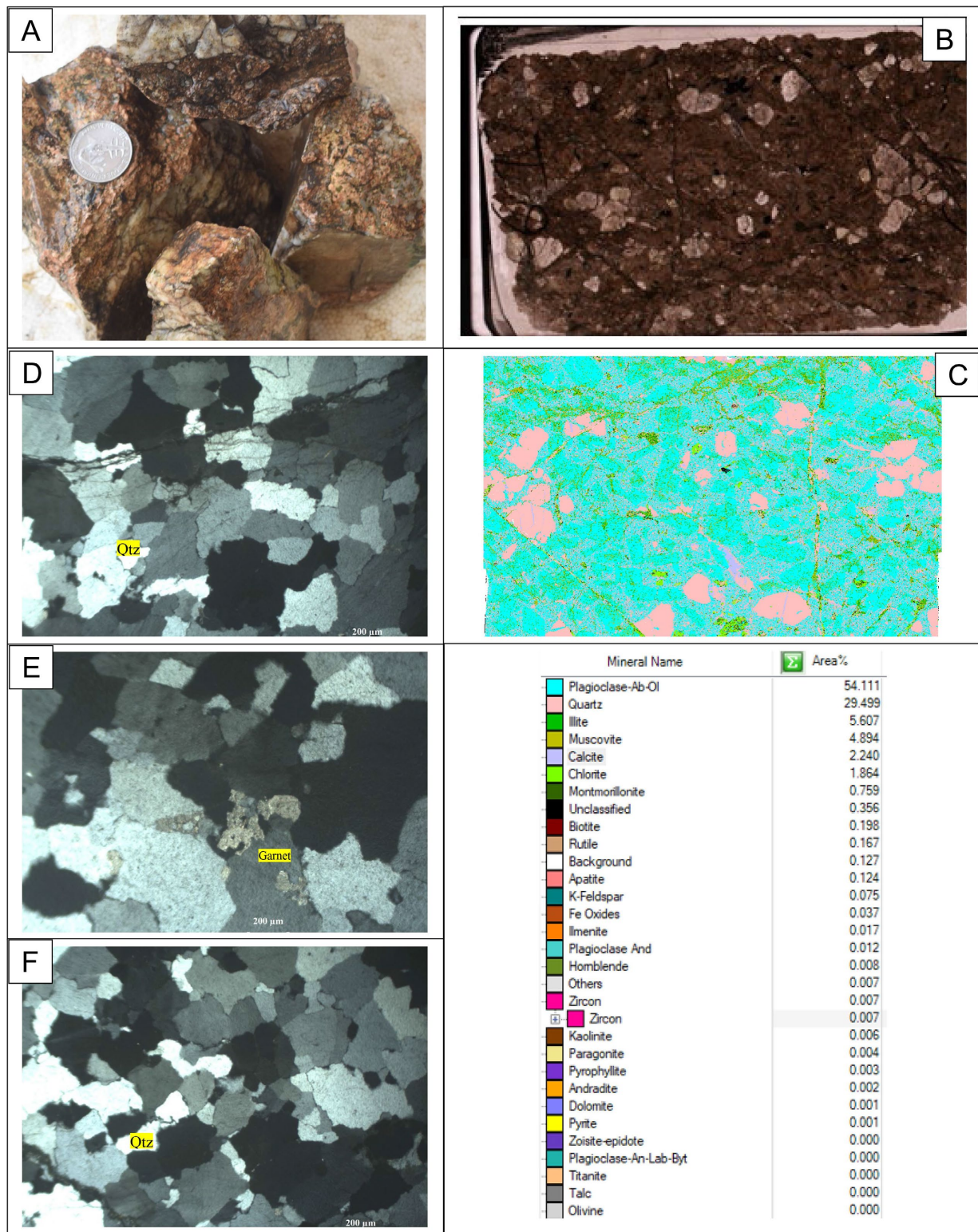


Figure 17. Facies of Tiguida pluton. A: Representative (sample 62) of Tiguida granite from outcrop; B, C, D: detail of microphotographs of granite (ech. 61) in polished section; E: QUESCAN analysis giving mineral composition of ech. 61: plagioclase-Ab-Ol (54.11%), Quartz (29.49%), Illite (5.60%), Muscovite (4.89%), Calcite (2.24%), Chlorite (1.86%); E, F, G, H: details of microphotographs of fractures on granite (ech. 62) in thin section and polarized light; Pl: plagioclase; Garnet (andradite); Opx: Orthopyroxen; Cpx: Clinopyroxen; Qtz: Quartz; Bio: Biotite.

Table 1. Summary of the geochemical characteristics of the formations of maco.

Sample (ech.) Number	Nature	Type of rock	Majors (%)		Traces (ppm)		
			SiO ₂	(Na ₂ O + K ₂ O)	(La/Yb)N	(La/Sm)N	(ΣREE)
70	Calc-alkaline	Basalt	56.96	5.54	<Ldd	2.79	81.9
89	Calc-alkaline	Basalt	57.07	5.17	1.59	<Ldd	50.8
63	Calc-alkaline	Diorite	58.99	3.45	<Ldd	1.74	38.8
90	Tholeiitic	Gabbro	52.06	3.47	2.02	1.17	64.6
88	Tholeiitic	Diorite	56.11	2.85	<Ldd	<Ldd	37
66	Calc-alkaline	Granite Dioudiokoukou	73.28	6.82	17.45	4.61	285.8

Volcanics represented by the calc-alkaline basalts have SiO₂ contents of between 56.96% and 57.07% and rare earth contents of between 50.8 and 81.9 ppm.

Plutonic formations are represented by calc-alkaline diorites, tholeiitic diorites and tholeiitic gabbros. The gabbros and tholeiitic diorites at Maco are slightly enriched in light rare earths, with a LaN/SmN ratio of between 1.17 and 1.74. The **Table 1** summarises the geochemical characteristics of the lithological samples (from Maco) on which the analyses were carried out.

5.5.2. Geochemical Signature of Sesam

The study (majors and traces) of the formations of Sesam lithostructural domain highlights three groups of magmatic rocks that may be tholeiitic or calc-alkaline (**Table 2**): these are volcanic formations, plutonic facies and volcanosedimentary facies.

Table 2. Summary of the geochemical characteristics of the formations of Sesam.

Sample (ech.) Number	Nature	Type of rock	Majors (%)		Traces (ppm)		
			SiO ₂	(Na ₂ O + K ₂ O)	(La/Yb)N	(La/Sm)N	(ΣREE)
18	Tholeiitic	Andesitic basalt	55.93	3.19	<Ldd	<Ldd	23.2
13	Tholeiitic	Andesite	54.89	4.41	1.44	1.16	46.3
3	Tholeiitic	Volcanosediment	72.59	1.05	<Ldd	<Ldd	34.4
21	Calc-alkaline	Andesite	59.44	4.58	<Ldd	<Ldd	32.3
15	Calc-alkaline	Volcanosediment	50.89	4.84	<Ldd	2.22	66.3
92	Calc-alkaline	Granodiorite Koulountou	64.46	4.24	3.54	1.94	111.3
59	Calc-alkaline	Granite Tiguida	72.48	6.89	<Ldd	<Ldd	28.7
97	Calc-alkaline	Granite Koulountou	67.75	7.47	<Ldd	2.55	176.6

Volcanics are represented by tholeiitic andesitic basalts, tholeiitic andesites and calc-alkaline andesites. The SiO₂ content of tholeiitic andesitic basalts and tholeiitic andesites varies between 54.89% and 55.93%. Rare earth contents 23.2 to 46.3.

Calc-alkaline andesites, on the other hand, have an SiO₂ content of 59.44% and

a rare earth content of 32.3. The volcanic rocks of the Sesam domain show a low enrichment of light rare earths with a LaN/SmN ratio equal to 1.16.

The plutonic formations are calc-alkaline and are mainly represented by the metal-bearing granodiorites of Sesam. They are moderately enriched in light rare earths, with a LaN/SmN ratio of between 1.94 and 2.55.

The volcanosedimentary facies of the Sesam domain show tholeiitic variety (ech3) with an alkaline content (Na₂O + K₂O) of 1.05% and a calc-alkaline variety with alkaline content (Na₂O + K₂O) of 4.84%.

The tholeiitic variety shows very low enrichment in light rare earths (LaN/SmN below the detection limit). The calc-alkaline variety shows average enrichment in light rare earths (LaN/SmN) ratio 2.22).

5.5.3. Geochemical Signature of Diabba

The chemical signature of formations of Diabba lithostructural domain are divided into three (3) tholeiitic and calc-alkaline magmatic groups (**Table 3**):

Table 3. Summary of the geochemical characteristics of Diabba formations.

Sample (ech.) Number	Nature	Type of roche	Majors (%)		Traces (ppm)		
			SiO ₂	(Na ₂ O + K ₂ O)	(La/Yb)N	(La/Sm)N	(ΣREE)
375	Tholeiitic	Basalt	47.63	4.31	11.09	3	122.4
76	Tholeiitic	Andesitic basalt	53.06	2.59	<Ldd	<Ldd	34.2
219	Calc-alkaline	Andesite	58.72	6.18	<Ldd	<Ldd	60.9
52	Calc-alkaline	Andesite	55.60	5.39	<Ldd	2.18	62.2
341	Calc-alkaline	Dacite	60.50	4.38	<Ldd	<Ldd	39.9
230	Calc-alkaline	Dacite	59.32	3.97	<Ldd	5.3	108.9
30	Detritic	Sediment	50.87	3.39	<Ldd	<Ldd	17.2
38	Chemical	Chert	76.40	6.98	0.87	0.88	40.9
81	Calc-alkaline	Granite Tinkoto	67.93	7.30	<Ldd	3.76	75.6
317	Calc-alkaline	Granodiorite Diabba	67.49	6.14	<Ldd	<Ldd	36

Volcanics are represented by tholeiitic basalts, tholeiitic andesitic basalts, calcoalkaline andesites and calcoalkaline dacites. The SiO₂ content of basalts and andesitic basalts varies from 47.63% to 53.06%.

Light rare earth contents are 122.4 for tholeiitic basalts and 34.2 for tholeiitic andesitic basalts. Calc-alkaline andesites and calc-alkaline dacites have SiO₂ contents 55.60 to 60.50. Light rare earth contents range from 60.9 to 62.2 for calc-alkaline andesites and from 39.9 to 108.9 for calc-alkaline dacites.

Volcanics of Diabba are enriched in light rare earths with a LaN/SmN ratio equal to 3 for tholeiitic basalts showing high fractionation rate with a LaN/YbN ratio of 11.7. The LaN/SmN ratio is 2.18 for calc-alkaline andesites and 5.3 for calc-alkaline dacites. Plutonics will be dealt in another sub-chapter.

The metasedimentary facies of Diabba domain show a variety (ech30) with an alkaline content ($\text{Na}_2\text{O} + \text{K}_2\text{O}$) of 1.05% and a variety with an alkaline content ($\text{Na}_2\text{O} + \text{K}_2\text{O}$) of 4.84%. The low alkali enriched variety has a low light rare earth content (ΣREE : 17.2) with a LaN/SmN ratio below the detection limit). Whereas the variety most enriched in alkalis is richer in light rare earths (ΣREE : 40.9) with a LaN/SmN ratio of 2.22.

5.6. Typologie of Magmatisms

Magmatism is marked by volcanic and plutonic episodes recorded in lithostructural domains at Maco, Sesam and Diabba. This magmatic evolution is expressed in several volcanic and plutonic episodes marked by the production of six tholeiitic phases from different sources and three distinct calc-alkaline volcanic phases.

5.6.1. Magmatic Episodes of Maco

Magmatic episodes show that Maco is mainly characterised by unimodal (calc-alkaline) volcanism: the Maco calc-alkaline1 series with a volcanic arc affinity.

Maco tholeiitic plutonism highlights two tholeiitic series from different sources: the Maco tholeiites1 (fractionated mantle diorite) from a high potassium mafic source (high potassium mafic rock), with a volcanic arc affinity and Maco tholeiites2 (gabbros) from a low-potassium mafic source with a volcanic arc affinity (Table 4, Table 5 and Figure 22).

Table 4. Calc-alkaline volcanism in the Mako-Diale transition zone.

Sample (ech.) Number	Rock Type	Zone	Nature	Tectonic domain	Genesis environment	Geodynamic environment	Geotectonic field
CALC-AKALINE VOLCANISM							
70	Calc-alkaline	Maco	Basalt	Active margin	compressive	(Volcanic arc Basalt)	Ocean Ridge and floor
89	Calc-alkaline	Maco	Basalt	Active margin	compressive	(Volcanic arc Basalt)	Orogenic
219	Calc-alkaline	Diabba	Andesite	Active margin	compressive	Island arc lavas	Orogenic
52	Calc-alkaline	Diabba	Andesite	Active margin	compressive	Island arc lavas	Orogenic
21	Calcoalcaline	Sesam	Andesite	Not specified	Not specified	Island arc lavas	Orogenic
341	Calc-alkaline	Diabba	Dacite	Active margin	compressive	Island arc lavas	Orogenic
230	Calc-alkaline	Diabba	Dacite	Active margin	compressive	Island arc lavas	Orogenic
15	Calc-alkaline	Sesam	Volcanosediment	Active margin	compressive	Island arc lavas	Ocean Ridge and floor

Calc-alkaline volcanism of Maco is based on a compressive geodynamic environment of an active margin associated with volcanic arc market by volcanic arc basalts (ech.89, ech.70). The calc-alkaline volcanism of Sesam sets as volcanosediments (ech.15) with island arc lavas affinity (in context of Ocean Ridge and floor and calc-alkaline andesites (ech.21) with island arc lavas affinity in orogenic context. Diabba calc-alkaline volcanism sits on active margin compressive geodynamic environment. It is associated with an island arc marked by calc-alkaline andesite (orogenic) island arc lavas and calc-alkaline dacites island arc lavas (orogenic). Sesam volcanosediments represent andesitic (explosive volcanic) deposited materiel with facies ranging from coarse to fine (ash) lithic elements.

Table 5. Tholeiitic plutonism in the Mako-Diale transition zone.

Sample (ech.) Number	Rock Type	Zone	Nature	Tectonic domain	Genesis environment	Geodynamic environment	Geotectonic field
THOLEIITIC PLUTONISM							
90	Tholeiitic	Maco	Gabbro	Intra-continent	(compressive to distensive)	Pre-plate collision	Volcanic arc granitoid (VAG)
88	Tholeiitic	Maco	Diorite	Active margin	compressive	Fractionates mantle	Volcanic arc granitoid (VAG)

The tholeiitic plutonism of Maco is marked by the presence of tholeiitic gabbros from an intra-continental source (pre-plate collision zone) and tholeiitic diorites from a mantle source (fractionate mantle zone). Maco's tholeiitic gabbros come from a mafic magmatic source with a low potassium content (Low K mafic rock). In contrast, the tholeiitic diorites of Maco are derived from a "High K mafic rock" mafic magmatic source with a high potassium content (Figure 20): diagram of Laurent et al. (2014). In summary, the Maco tholeiitic plutonism highlights two tholeiitic series from different sources.

Table 6. Calc-alkaline plutonism of Mako-Diale transition zone.

Sample (ech.) Number	Rock Type	Zone	Nature	Tectonic domain	Genesis environment	Geodynamic environment	Geotectonic field
CALC-ALKALINE PLUTONISM							
63	Calc-alkaline	Maco	Diorite	Intra- continent	(compressive to distensive)	Fractionates mantle	Volcanic arc granitoid (VAG)
92	Calc-alkaline	Sesam	Granodiorite Koulountou	Intra- continent	(compressive to distensive)	Fractionates mantle	VAG + Syn COLG
317	Calc-alkaline	Diabba	Granodiorite	Active margin	compressive	Pre-plate collision	VAG + Syn COLG
81	Calc-alkaline	Diabba	Granite Tinkoto	Active margin	compressive	Pre-plate collision	VAG + Syn COLG
59	Calc-alkaline	Sesam	Granite Tiguida	Active margin	compressive	Syn-collisionnel	VAG + Syn COLG
97	Calc-alkaline	Sesam	Granite Koulountou	Active margin	compressive	Post-collision uplift	VAG + Syn COLG – WPG – ORG
66	Calc-alkaline	Maco	Granite Dioudiokoukou	Active margin	compressive	Post-orogenic	VAG + Syn COLG – WPG – ORG

The Maco calc-alkaline plutonism is represented by the Maco diorite (ech.63) associated with a geodynamic environment of volcanic arc granitoids (VAG). There is also the Dioudiokoukou (ech.66) orogenic granite. The Sesam calc-alkaline plutonism is underlain by two geodynamic environments: compressive and a compressive to distensive active margin. It is associated with volcanic arc granitoids and intraplate granitoids (WPG): The volcanic arc granitoids (VAG) are calc-alkaline, in active margin context and orogenic (compressive). They correspond to the Koulountou granodiorites (ech.92) and the Tiguida granite (ech.59); the WPG intraplate granitoids are calc-alkaline, active margin and orogenic (compressive). They are represented by calc-alkaline Koulountou granite (ech.97). The calc-alkaline Diabba plutonism is based on compressive active margin geodynamic environment associated with volcanic arc granitoids (by Tinkoto granite (ech.81) and Diabba granodiorite (ech.317).

5.6.2. Magmatic Episodes of Sesam

The magmatism of the Sesam arc is marked by MORBs tholeiites associated with arc tholeiites and calc-alkaline series (Table 4, Table 6, Table 7 and Figure 22): tholeiites3 of Sesam (ech.18: andesitic basalt) with MORBs affinity from active margin (Ocean Ridge and floor), tholeiites4 of Sesam (ech.13: andesite) with intracontinental MORBs affinity (Spreading center of island) and tholeiites with insular arc lavas affinity (ech.3 volcanosediments) and calc-alkaline2 series of Sesam with insular arc affinity fed by two sources with distinct geotectonic

contexts (ech.21: andesite in orogenic context and ech.15: volcanosediment with insular arc affinity in Ocean Ridge and floor context).

Table 7. Tholeiitic volcanism.

Sample (ech.) Number	Rock Type	Zone	Nature	Tectonic domain	Genesis environment	Geodynamic environment	Geotectonic field
THOLEITIC VOLCANISM							
375	Tholeiitic	Diabba	Basalt	Active margin	compressive	Within plate lavas	Continental
18	Tholeiitic	Sesam	Andesitic basalt	Active margin	compressive	MORBs	Ocean Ridge and floor
76	Tholeiitic	Diabba	Andesitic basalt	Active margin	compressive	MORBs or OIBs	Ocean island
13	Tholeiitic	Sesam	Andesite	Intra-continental	(compressive to distensive)	MORBs	Spreading center of island
3	Tholeiitic	Sesam	Volcanosediment	Active margin	compressive	Island arc lavas	Spreading center of island

Tholeiitic volcanism manifests itself in tectonovolcanic episodes belonging to very distinct geodynamic environments: Intraplate basalts (intraplate lavas) with an affinity for MORBs (ech.375 = Diabba basalt); Andesitic basalts (ech.76 = Diabba andesitic basalt) of active (compressive) margin with MORBs or OIBs affinity; Intracontinental (compressive to distensive) andesites (ech.13 = Sesam andesite) with MORBs intraplate affinity; active margin andesitic basalts (ech.18 = Sesam andesitic basalt) with an affinity for island arc lavas; active margin (compressive) tholeiitic volcanosediments (ech.3=Volcanosediments de Sesam) with affinity for island arc lavas. Sesam volcanosediments represent andesitic (explosive volcanic) deposited material with facies ranging from coarse to fine (ash) lithic elements.

5.6.3. Magmatic Episodes of Diabba

The Diabba domain is marked by tholeiitic volcanisms and calc-alkaline volcanisms (Table 4, Table 6, Table 7 and Figure 22): *Diabba tholeiites5* (basalt) with affinity for intraplate lavas (continental zone); *Diabba tholeiites6* (andesitic basalt) with MORBs or OIBs affinity (oceanic islands zone) and Diabba calc-alkaline series3 (andesites) with island arc affinity (orogenic).

5.6.4. Magmatic Episodes of Calc-Alkaline Plutonic Masses

Six tholeiitic series are associated with six major calc-alkaline plutonic masses (Tables 1-3, Table 6 and Figure 22):

- 1) Dioudiokoukou post-orogenic calc-alkaline granite
- 2) Koulountou post-collision uplift calc-alkaline granite
- 3) Tiguida Syn-orogenic calc-alkaline granite
- 4) Preplate collision calc-alkaline granite at Tinkoto
- 5) Diabba calc-alkaline granodiorite (preplate collision)
- 6) Koulountou calc-alkaline granodiorite (fractionate mantle)

These large plutonic masses belong to three (3) different magmatic sources: Koulountou (ech.97) and Tinkoto granites and Koulountou granodiorite come from high-K mafic sources while Tiguida granite and Diabba granodiorite are issued from low-K mafic rocks. Dioudiokoukou granite belongs to tonalite source.

5.7. Magmatism and Orogenic Tectonism

Tectonism is the set of movements that affect the Earth's crust and cause the

deformation, reorganisation or break-up of rock layers. Orogenic tectonism is when movements occur horizontally giving rise to mountains and areas with folds and faults. The results of the work highlight complexes marked by magmatism and backed by orogenic tectonism. These are known as tectonomagmatic complexes. The tectonomagmatic complexes consist of volcanoplutonic formations with distinct geodynamic environments associated with three (3) major tectonic boundaries: CiscoW, CiscoM and CiscoE. These tectonomagmatic complexes are the Maco oceanic crust, the Sesam arc and the Diale back-arc-basin.

5.7.1. Maco Oceanic Crust

It extends from the pre-plate collision zone to the Maco orogenic zone via the ridge zone and the seafloor. The Maco oceanic crust is bounded to the East by the CiscoW shear-contact zone. It is characterized by the production of orogenic late to post-orogenic mafic magmas, mainly represented by calc-alkaline basalts, tholeiitic gabbros and diorites, calc-alkaline diorites and the Dioudiokoukou granite. Calc-alkaline active margin basalts shows volcanic arc affinity. These formations of Maco oceanic complex are intersected by peraluminous (Figure 20), post-orogenic intraplate granite of Dioudiokoukou. Maco volcanism is calc-alkaline (Figure 18) in a subduction context. It is associated with two tholeiitic series: Maco tholeiites1 and tholeiites2 from distinct mafic sources (Figure 21).

5.7.2. Sesam Arc

Sesam arc extends from the CiscoW shear-contact zone to the interface between the orogenic domain and that of the oceanic islands adjacent to the spreading oceanic ridge. Sesam volcanic arc is marked by basic to intermediate orogenic, syn-collisional to post-collisional uplift volcanism, mainly marked by tholeiitic andesitic basalts, tholeiitic and calc-alkaline andesites and tholeiitic and calc-alkaline volcano sediments. These volcanic and volcanosedimentary formations are intersected by the metaluminous, syn-collisional Tiguida granite and by the two plutonic episodes of the compressive active margin of Koulountou: the first represented by the calc-alkaline granodiorites from “fractionates mantle” zone and the second by the post-collisional, metaluminous (Figure 20) uplift granite of Koulountou. The magmatism of the arc is marked by two tholeiitic series associated with a calc-alkaline series: Sesam tholeiites3 with MORBs affinity, Sesam tholeiites4 with MORBs affinity (Figure 19), Sesam arc tholeiites and Sesam calc-alkaline2 series with island arc affinity.

5.7.3. Diale Back-Arc Basin (Diabba)

Diale back-arc basin extends from the arc domain to the continent. It is bounded to the West by the CiscoM shear-contact zone. These tectonovolcanic episodes are intersected by the calc-alkaline, peraluminous Diabba granodiorite and the calc-alkaline, metaluminous Tinkoto granite associated with orogenic island arc lavas. Sediments are associated with the continental domain. Sedimentary facies are essentially anorogenic (cherts) and detrital (fine metasediments) setting on volcanics. Diabba back-arc basin is marked by two distinct tholeiitic series associated

with a calc-alkaline series: Diabba tholeiites5 with MORBs intraplate affinity and Diabba tholeiites6 with MORBs or OIBs affinity (Figure 19) and Diabba calc-alkaline series3 with an island arc affinity.

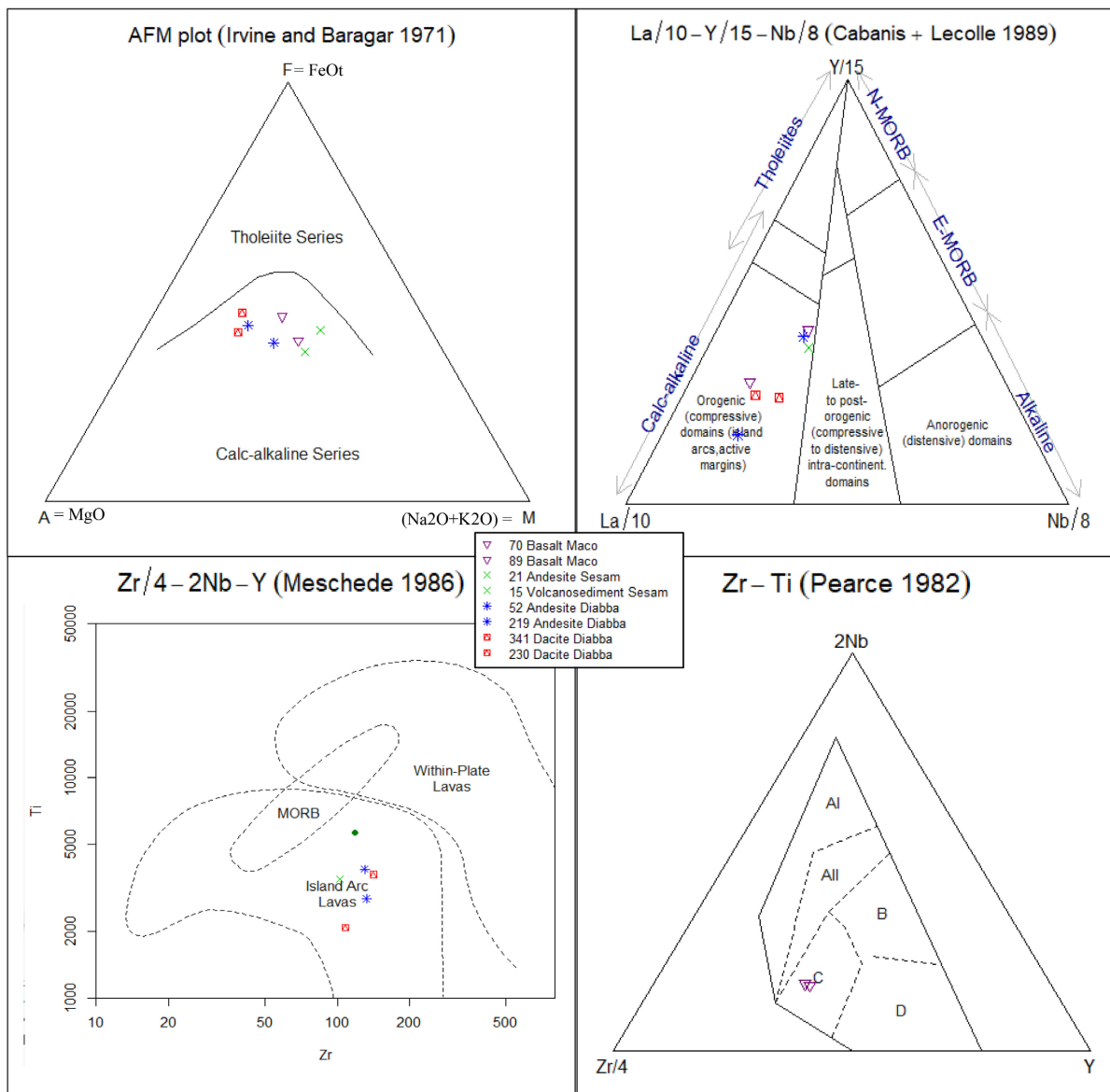


Figure 18. Geochemical signature of calc-alkaline volcanics. AFM diagram of *Irvine and Baragar (1971)* showing the volcanic affinity of the rocks of the ZTMD; La/10-Y/15-Nb/8 ternary diagram of *Cabanis and Lecolle (1989)* applied to the volcanic rocks of the ZTMD; Th/Yb-Ta/Yb diagram of *Pearce (1982)* applied to the intermeiary and acid calcoalkaline volcanic rocks of the ZTMD; *Meschede (1986)* applied to Maco basalts; AI-AII = Within-Plate Alkaline Basalts, AII-C = Within-Plate Tholeiites, B = P-type Mid-Ocean Ridge Basalts, D = N-type Mid-Ocean Ridge Basalts and C-D = Volcanic Arc Basalts; ZTMD = transition zone of Mako-Diale, diagram by *Pearce and Gale (1977)* and Th/Yb-Ta/Yb diagram by *Pearce (1982)* applied to basic and intermediate rock. The combined diagrams show that Maco's calc-alkaline volcanism is based on a compressive active margin associated with a volcanic arc. It is characterised by the presence of volcanic arc basalts (ech.89, ech.70). The calc-alkaline volcanism of Sesam set as volcanics belonging to an island arc environment associated with: calc-alkaline volcanosediments with an affinity for island arc lavas (ech.15); and calc-alkaline andesites with affinity for island arc lavas (ech.21). The calc-alkaline volcanism of Diabba sets in compressive active margin. It is associated with an island arc represented by island arc lavas (ech.52; ech.218); and island arc lavas (ech.341; ech.230).

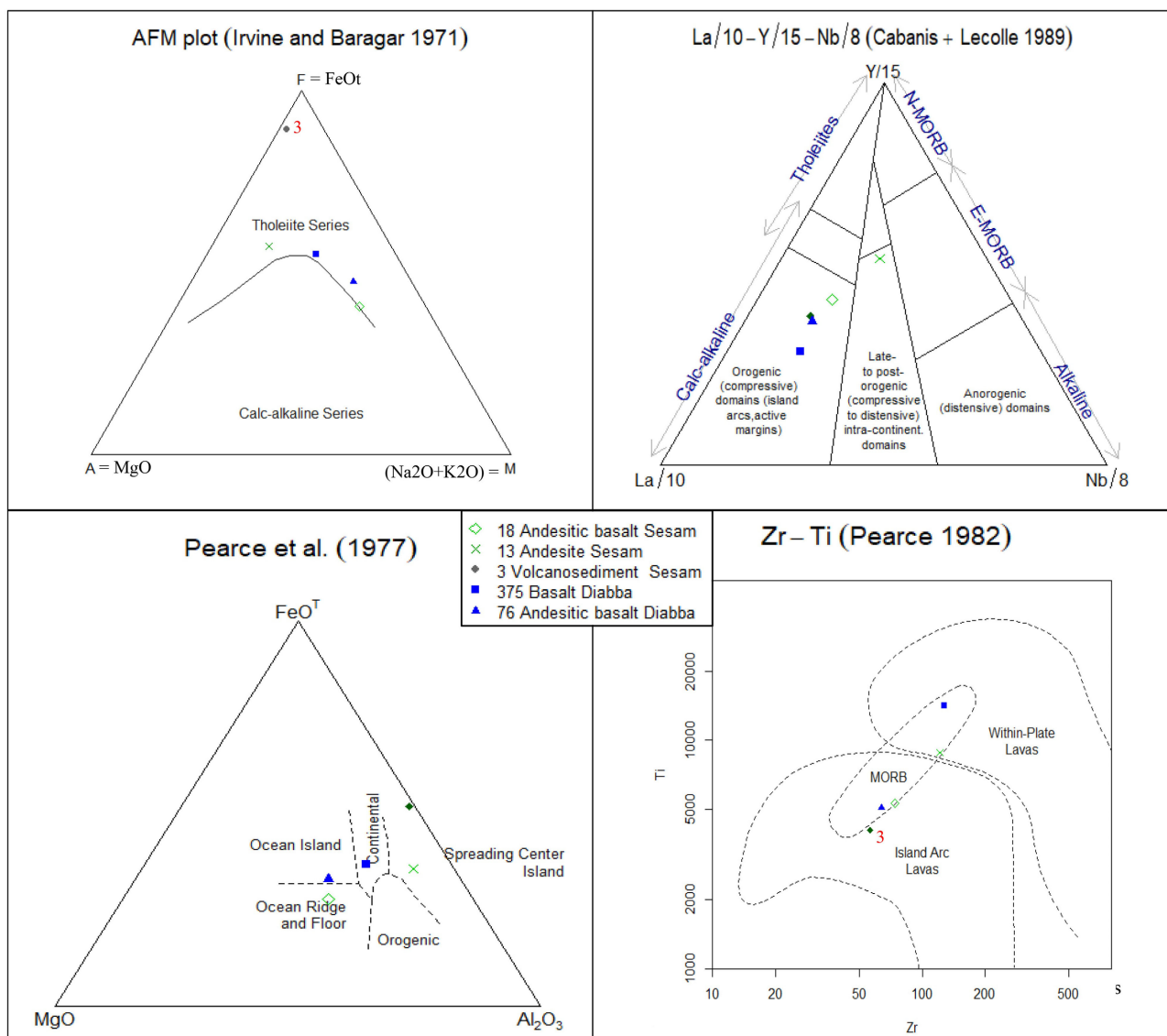


Figure 19. Geochemical signature of tholeiitic volcanics. AFM diagram of *Irvine and Baragar (1971)* showing the volcanic affinity of the rocks of the ZTMD; La/10-Y/15-Nb/8 ternary diagram of *Cabaniş and Lecolle (1989)* applied to the volcanic rocks of the ZTMD; Th/Yb-Ta/Yb diagram of *Pearce (1982)* applied to the intermeiary and acid calcoacaline volcanic rocks of the ZTMD; *Meschede (1986)* applied to Maco basalts; AI-AII = Within-Plate Alkaline Basalts, AII-C = Within-Plate Tholeiites, B = P-type Mid-Ocean Ridge Basalts, D = N-type Mid-Ocean Ridge Basalts and C-D = Volcanic Arc Basalts. AFM diagram by *Irvine and Baragar (1971)* showing the magmatic affinity of rocks; La/10-Y/15-Nb/8 ternary diagram by *Cabaniş and Lecolle (1989)*; diagram by *Pearce and Gale (1977)* and Th/Yb-Ta/Yb diagram by *Pearce (1982)* applied to basic and intermediate rock. The diagram by *Pearce and Gale (1977)* shows that the tholeiitic andesitic basalts of Sesam (ech.18) are in the ‘Ocean ridge and floor’ field. The tholeiitic andesites (ech.13) of Sesam have MORB affinity in context of Spreading Center of Island. The Diabba tholeiitic andesitic basalts are found in the Ocean island field, while the Diabba tholeiitic basalts (ech.375) are found in the continental domain. The volcanosediments (ech.3) of Sesam are in the “Spreading Center of Island” field and are tholeiites. Pearce’s diagram (*Pearce, 1982*) shows that the tholeiitic basalts (ech.375) are Mid-oceanic ridge basalt MORBs with an affinity for Within plate lavas. The andesitic basalts of Sesam (ech.18) are Mid-oceanic ridge basalt (MORBs) with an affinity for island arc. The andesitic basalts of Diabba (ech.76) are Mid-oceanic ridge basalt (MORBs) or Ocean Island basalt (OIBs) with island arc. The Sesam volcanosediments (ech.13) are arc tholeiites showing an affinity with island arc lavas. Sesam volcanosediments represent andesitic (explosive volcanic) deposited materiel with facies ranging from coarse to fine (ash) lithic elements.

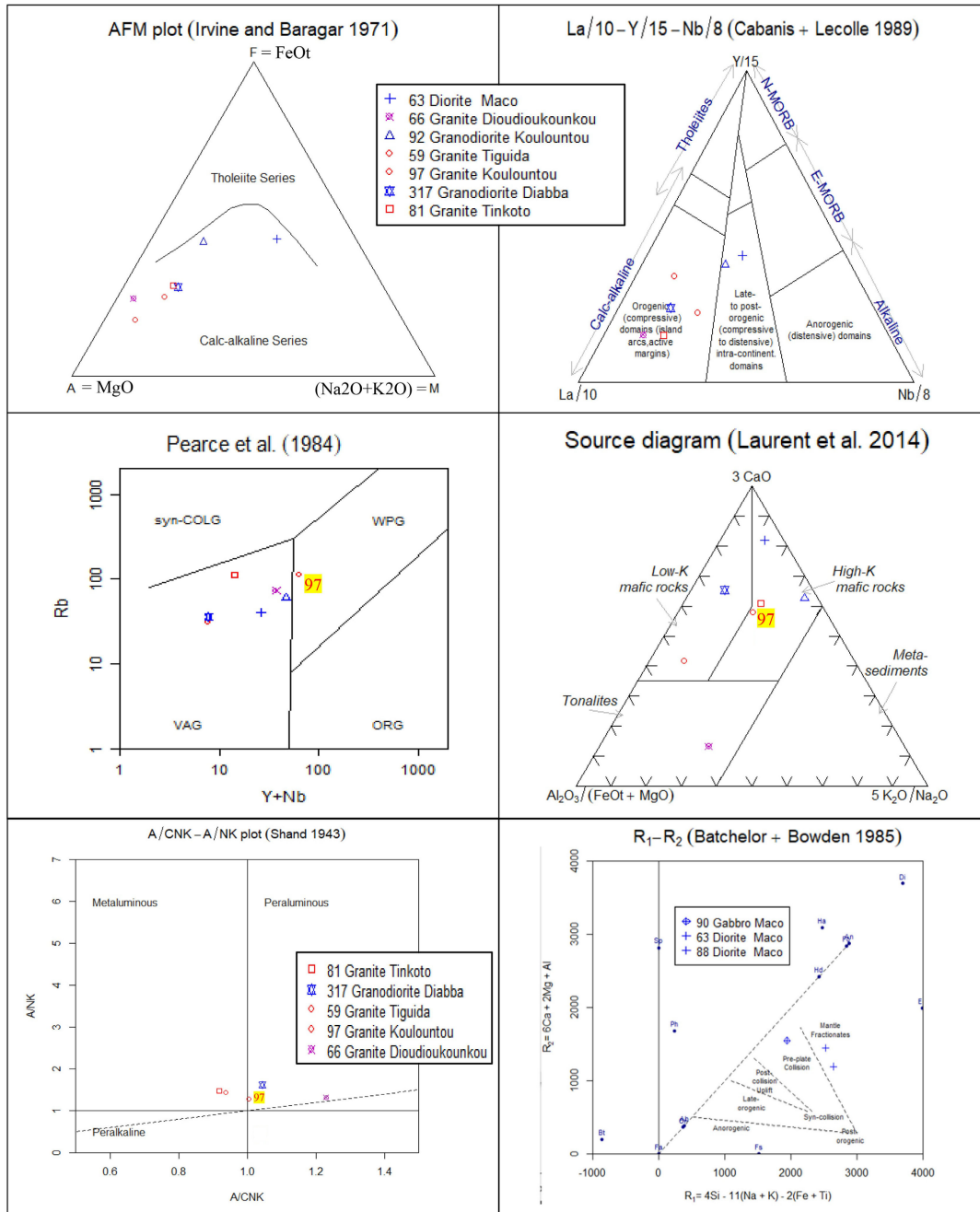


Figure 20. Geochemical signature of calc-alkaline large plutonic masses. The AFM diagram of *Irvine and Baragar (1971)* distinguishes a single magmatic series for large plutonic masses: the calc-alkaline series represented by Koulountou granite (ech.97), Tiguida granite (ech.59), Tinkoto granite (ech.81), Dioudioukounkou granite (ech.66), Diabba granodiorite (ech.317), Maco diorite (ech.63) and Diabba granodiorite (317); *Shand (1943)* diagram applied to large plutonic masses of Mako-Diale transition zone shows that three (3) facies are peraluminous and correspond to the following samples: sample 66 from the Maco domain, sample 59 from the Sesam domain and sample 317 from Diabba domain. The other two (2) facies are metaluminous. They correspond to Tinkoto (sample 81) and Koulountou (sample 97) granites belonging respectively to Diabba and Sesam domains. The *Batchelor and Bowden (1985)* diagram applied to granitoids shows that tholeiitic gabbros are in the 'pre-plate collision' zone. On the other hand, the tholeiitic diorites (ech.88) and calc-alkaline diorites (ech.63) of Maco are in the 'fractionate mantle' field. The diagram of *Laurent et al. (2014)* shows that large plutonic masses belong to three (3) different sources: Koulountou (ech.97) and Tinkoto granites are sourced from high-K mafic rocks, while Tiguida granite and Diabba granodiorite belong to low-K mafic rocks. The Dioudioukounkou granite is sourced from tonalitic rocks.

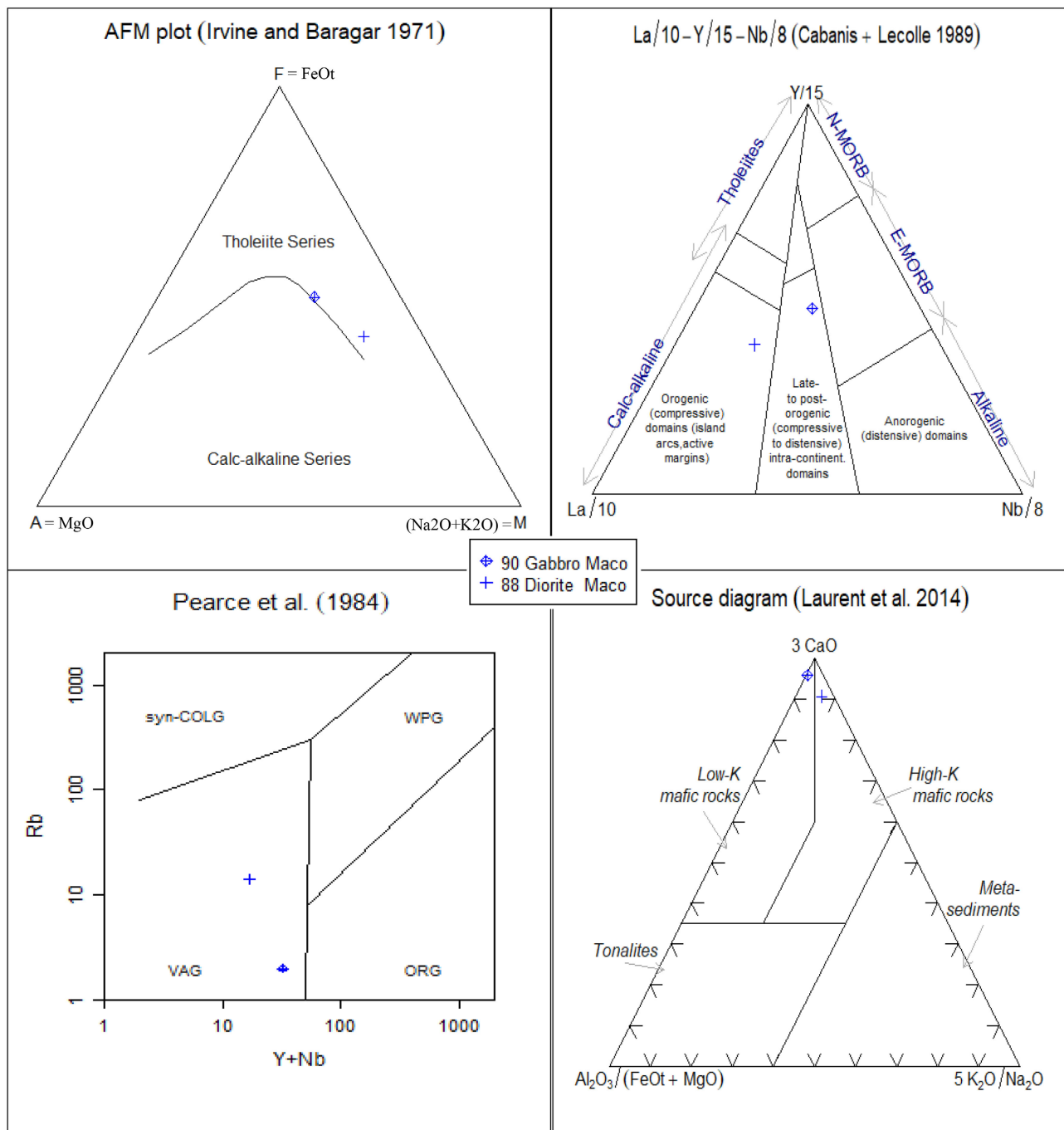


Figure 21. Geochemical signature of tholeiitic plutonism of Maco. The AFM diagram of Irvine and Baragar (1971) shows that tholeiitic plutonism is represented by the gabbros (ech.90) and diorites (ech.88). The diagram by Laurent et al. (2014) shows that tholeiitic plutonism of Maco domain is marked by the presence of tholeiitic gabbros from an intra-continental source (pre-plateau collision zone) and tholeiitic diorites from a mantle source (fractionate mantle zone). Maco's tholeiitic gabbros come from a mafic magmatic source with a low potassium content (Low K mafic rock). The tholeiitic diorites of Maco are derived from a mafic magmatic source with a high potassium content (High K mafic rock). In short, Maco's tholeiitic plutonism highlights two tholeiitic series from different sources. The diagram of Pearce et al. (1984) applied to the basic to intermediate plutonic formations of Maco shows that the tholeiitic gabbros, tholeiitic diorites and calc-alkaline diorites are in the volcanic arc granitoids (VAG) zone. The Batchelor and Bowden (1985) diagram applied to granitoids shows that tholeiitic gabbros are in the "pre-plate collision" zone. The tholeiitic diorites (ech.88) and calc-alkaline diorites (ech.63) of Maco are in the "fractionate mantle" field.

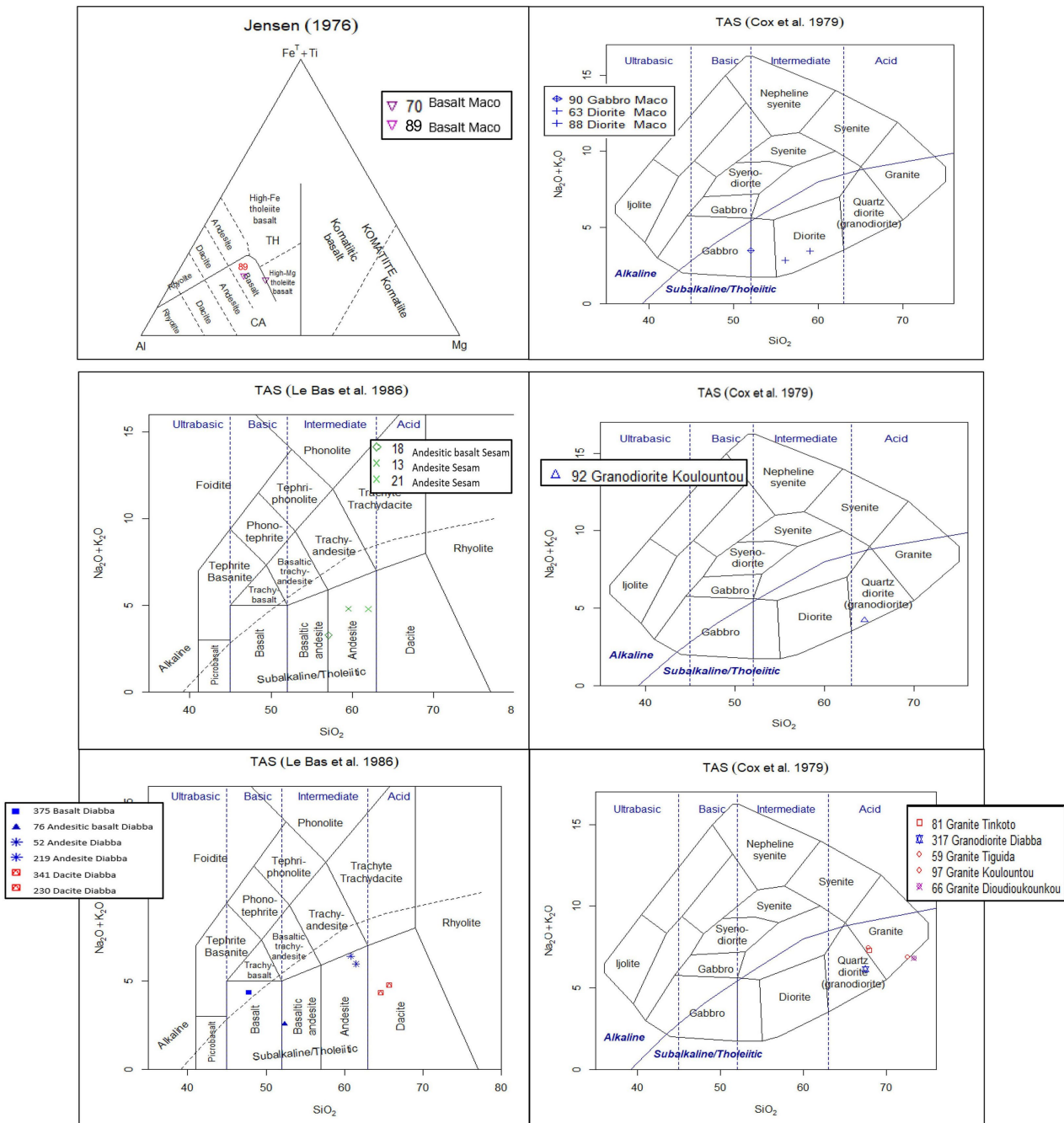


Figure 22. Classification of the formations of the Mako-Diale transition zone. **Jensen (1976)** applied to volcanics shows that samples 89 and 70 are calc-alkaline basalts. Sample 89 is massive and associated with the Maco domain. Sample 70 is an enclave basalt in the Dioudioukounkou granite, thus belonging to the Maco domain. The classification of volcanic facies of Sesam is defined with TAS (**Le Bas et al., 1986**) diagram showing that Sesam volcanics are essentially formed by andesitic basalts (ech.18) and andesites (ech.13, ech.21). The TAS diagram (**Cox et al., 1979**) shows that plutonic formations (apart from the large plutonic masses) of Sesam are mainly composed of acid facies. These are quartz-bearing diorites or granodiorites (ech.92). The diagram of **Le Bas et al. (1986)** shows that volcanic formations of Diabba are essentially formed of basalts (ech.375), andesitic basalts (ech.76), andesites (ech.52, ech.219) and dacites (ech.341, ech.219).

6. Discussions

The Mako-Diale transition zone is represented by the interface between the volcanic belt and Diale sedimentary basin. Aeromagnetic and cartographic data show that lithologies of Mako-Diale transition zone are composed of greenstone mainly represented by basic, intermediate to felsic volcanics associated with metasediments and metavolcanosediments. The contours of the granitoids were redefined using radiometric and cartographic data. The geophysical, geochemical and structural results of lithostructural domains were used to build new architecture for Mako-Diale transition zone. Mako is divided into three domains: Maco, Sesam and Diabba.

6.1. Discussion on Tectonic and Magmatic Contexts

The characterisation of magmatism and orogenic tectonism enable to define the geodynamic evolution of lithostructural domains within Mako-Diale transition zone into tectonomagmatic complexes (Maco Oceanic crust, Sesam Arc and Diale back-arc-basin) associated with three major shears: the Western Shear-Contact Zone (CiscoW corresponding to Sabodala Shear: SSZ), the Middle Shear-Contact Zone (CiscoM) and the Eastern Shear-Contact Zone (CiscoE corresponding to Main Transcurrent shear Zone: MTZ).

The discovery of the CiscoM and Diabba raises the question of the lithostructural definition of the major shear zones of Mako. The boundary between Mako and Diale-Dalema supergroups, which had previously been established to the MTZ mapped by [Ledru et al., 1988](#), was redefined in this study. The new boundary is marked by the median shear-contact CiscoM. The Yaakar Transcurrent shear zone, defined by [Sow \(2004\)](#) at the contact of volcanic, volcanosedimentary and sedimentary formations and forming a shear corridor with the MTZ, could have been comparable to the CiscoM, except that the latter (the CiscoM) is formed by a main branch oriented North-south to North-east associated with second-order structures. The MTZ remains the eastern lithostructural limit of the volcanoclastic formation along Massawa deposit located within Diale back-arc-basin. It constitutes a dextral shear zone oriented North-east to locally North-south formed by a continuous main branch (0,3 meter wide) over the entire area of study and by subparallel, discontinuous second-order structures. Taking these characteristics into account, the discontinuous model of MTZ from [Diene et al. \(2012\)](#) showing a western branch and an eastern branch with ponytail branches to the South seems out of step with the evidence continuity of CiscoE along its main branch associated with subparallel second-order structures observed to the East of entire area of study.

6.2. Discussion on Geochemical Context

Maco volcanism is unimodal (calc-alkaline) and marked by the production of volcanic arc basalts in a subduction context. This result confirms the consensus of several authors ([Bassot, 1987](#); [Dia, 1988](#); [Boher et al., 1992](#); [Sylvester & Attoh, 1992](#); [Diallo, 1994](#); [Dioh, 1995](#); [Ama Salah et al., 1996](#); [Béziat et al., 2000](#); [Mous-solo, 2000](#); [Diallo, 2001](#); [Lahondere et al., 2002](#); [Pawlig et al., 2006](#); [Sangare, 2008](#);

Dioh et al., 2006; Theveniaut et al., 2010; Gozo et al., 2015) showing geodynamic evolution of the calc-alkaline series which is associated with a volcanic arc formed in a context of subduction with the only difference that these authors consider all of Mako as homogeneous framework. On the contrary, this study defines Mako as heterogeneous lithostructural framework formed by three lithostructural domains, including Maco located to the West of CiscoW = Sabodala shear zone. Maco is therefore not Mako.

The context of tholeiites has long been debated, and several reference models have been proposed by authors at the Kedougou Inlier scale within the West African craton. Ngom, 1995; Ngom et al., 2007; Theveniaut et al., 2010; argued in favour of a MORB context at Mako, while Zonou, 1987 proposed an N-MORB context at Bouroum-Nord in Burkina Faso. Dia, 1988; Diallo, 2001; Pawlig et al., 2006 support the idea of an arc environment at Mako, as do Ama Salah et al. 1996 at Liptako in Niger; Beziat et al. 2000 at Loraboue and Baratoux et al., 2011 at Boromo and Hounde in Burkina Faso; Sangare, 2008 at Kadiolo in Mali and Sylvester and Attoh, 1992; Attoh et al., 2006; Dampare et al., 2008, 2009, 2019 at Ashanti in Ghana). Dioh (1995) argues in favour of a transition between MORB and arc while Dabo et al., 2017 support a MORB or OIB context for the geodynamic formation of the Mako tholeiites.

More recently, Labou, 2019; Labou et al., 2020 highlight a dual tholeiitic series with tholeiites1 and tholeiites2 from different sources corresponding to two different geodynamic contexts. The tholeiitic1 has signatures comparable to MORBs, while the tholeiitic2 and the calc-alkaline are compatible with series emplaced in an arc environment. This result defined by Labou, 2019; Labou et al., 2020, which puts data from Lame, Sofia and Koulountou (located to the South-western continuity of the Sesam domain) into the same analysis grid for basic and ultrabasic rocks, is confirmed by our study. However, this result cannot be extended to all Mako representing the volcanic belt integrating Diale basin (this study shows that lithostructural architecture of Mako is made up of three domains: Maco, Sesam and Diabba). Consequently, the tholeiites with signature comparable to MORBs associated with arc tholeiites and the arc calc-alkaline series (Labou, 2019; Labou et al., 2020) corresponds to a partial signature of one domain of Mako. It could be comparable to the result described by Dioh (1995) in favour of a transition between MORBs and arc.

This result is typical of the only Sesam domain associating **tholeiites3** (**tholeiites1** and **tholeiites2** are already cited in Maco) from Sesam with active margin MORBs affinity (Ocean Ridge and floor), **tholeiites4** from Sesam with intracontinental MORBs affinity (Spreading centre of island), island arc tholeiites and the calc-alkaline2 from Sesam with island arc affinity (this study). Sesam **calc-alkaline2** series with island arc affinity is comparable to island arc model (Dia, 1988; Pawlig et al., 2006) which suggests lithospheric convergence leading to subduction. This island arc context is also comparable to that already described in the Mako Group by Dia (1988), Diallo (2001) and Pawlig et al. (2006) and in the West

Africa Craton, in particular at Liptako in Niger by [Ama Salah et al. \(1996\)](#); at Loraboue in Burkina Faso by [Beziat et al. \(2000\)](#) and at Kadiolo in Mali by [Sangare \(2008\)](#).

The context of **tholeiites5** (continental basalts) with intraplate MORBs affinity and **tholeiites6** with MORBs or OIBs affinity is comparable to that of [Dabo et al. \(2017\)](#) who support a MORBs or OIBs context for the geodynamic setting of Mako tholeiites. Diabba tholeiites5 and tholeiites6 are associated with the **calcoalkaline3** series (andesite and dacite) with island arc affinity (orogenic). The context of continental diabba tholeiites5 with intraplate MORBs affinity (basalts) has been evoked in the Perkoa series in Burkina-Faso. The tholeiitic volcanism associated with the subgrauwacke sediments is interpreted as continental basalts emplaced under platform conditions on a continental basement ([Ratomaharo et al., 1988](#)). The production of continental basalts in favour of CiscoM rifting in Diabba domain (as defined in this study) has been described at the scale of the West African Craton. In fact, volcanism with an affinity for continental basalts in the Bouroum path was set up in favour of intracontinental rifting according to Kroner's model. The generation of the volcanic arc and then the island arc with island arc tholeiites (LATs) at the edge of the continent shows the evolution of the rift into a back-arc-basin. This environment is comparable to that described in the Upper Comoe, where isotopic data from the LATs and MORBs basalts suggest that the rift evolved into back arc basin in association with an island arc environment ([Lemoine, 1988](#)).

6.3. Discussion on Geodynamic Evolution

In summary, magmatic differentiation associated with the end of CiscoW would have led to the production of basic to intermediate terms of the Maco volcanic arc complex. This stage of the volcanic arc was followed by tectonic accretion of the Mako belt during the Eburnian orogeny [Kone et al. \(2020\)](#). The deformation phase D1 linked to crustal thickening ([Gueye & Ngom, 2020](#)), corresponds to the mylonitic contact shear zone CisoW corresponding to the Sabodala ductile transcurrent and sinistral shear zone (SSZ) oriented North-South to North-East and recorded between Koulountou pluton and the basaltic facies. CiscoW corresponds to D1. The D1 phase is dated at 2100 Ma ([Ledru et al., 1988](#)) and defined as a thrust ([Feybesse et al., 1989](#); [Ledru et al., 1988, 1991](#); [Milési et al., 1992](#)) or a periplutonic deformation ([Pons et al., 1995](#); [Vidal et al., 1996](#); [Debat et al., 2003](#); [Pitra et al., 2010](#); [Delor et al., 2010](#)).

This D1 phase is followed by the CiscoM, which separates Sesam island arc from the continental arc. At the end of the CiscoM, tectonics favoured a distension phase leading to tectonomagmatic complex (**Figure 23**) evolving toward the initiation of Diabba continental back-arc graben associated with the volcanic arc and epicontinental island arc complexes. Plutonic and volcanic formations in context of volcanic arc must have been locally uplifted and eroded to provide the main sedimentary input to the Diale basin. The Mako belt is the main source of detritus in the Diale-Dalema series. The dominant ages in the Diale-Dalema series range

from 2200 to 2100 Ma (Kone et al., 2020). D2 phase is the early Eburnean event which involves a sinistral transpressive deformation (Dabo et al., 2018). The opening of Diale back-arc-basin is linkable to CiscoM corresponding to D2 Phase dated 2096 Ma (Feybesse et al., 1989). D2 is transcurrent and associated with sinistral submeridian shears. It is a transcurrent to transpressive deformation, responsible for Eburnian tectonics marked by major NS to NE structures and plutonic intrusions into Proterozoic terrains (Ledru et al., 1988, 1991; Liégeois et al., 1991; Pons et al., 1995).

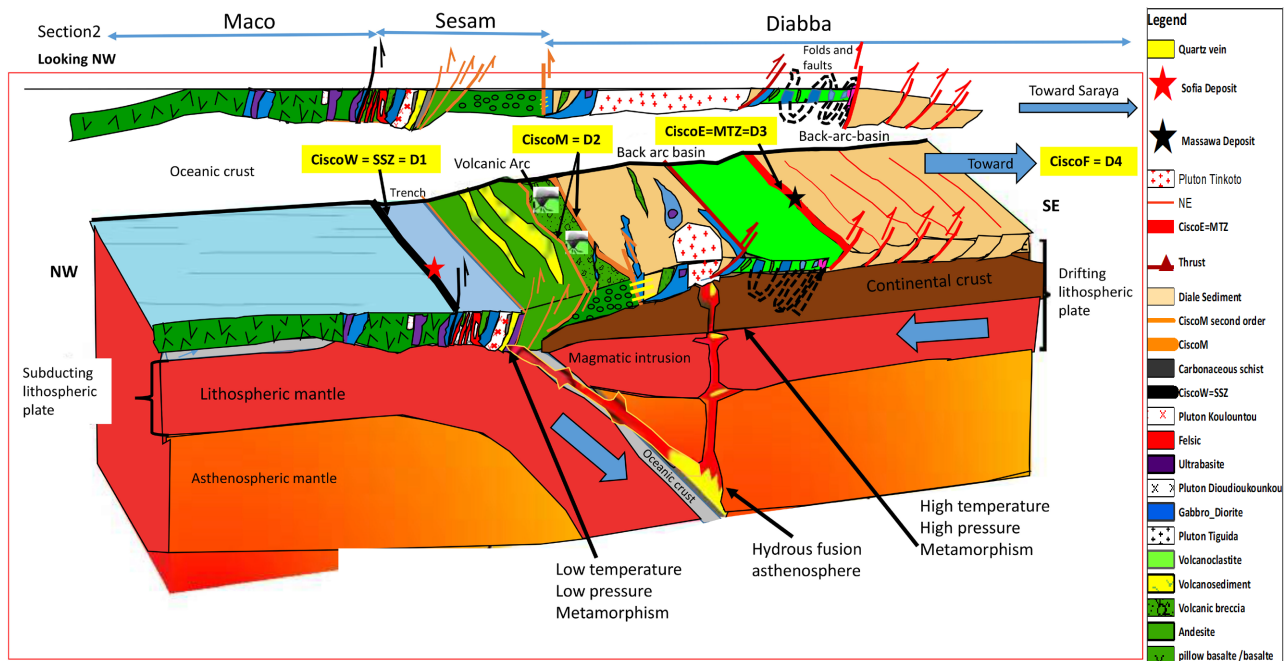


Figure 23. 3D model and 2D section of Tectonomagmatic complexes of Mako-Diale transition zone.

The phase D2 (CiscoM) is followed by CiscoE corresponding to D3. The D3 phase is marked by a series of East-north-east dextral detachments (Feybesse et al., 1989). Its manifestations have been found in Guinea, southern Mali and Côte d'Ivoire (Feybesse et al., 1989) and on the borders of Ghana and Côte d'Ivoire (Ledru et al., 1988). It is coaxial and marked by subvertical crenulation schistosity S3 N50° to N70° and straight P3 folds.

In Mako Supergroup, the late magmatic phase due to tardive deformation occurred between 2100-2070 Ma - Gueye et al. (2008). Eburnian magmatism ceased in the Mako belt after the Eburnian compressive deformation (Gueye et al., 2008) accompanied by the emplacement of the Tinkoto and Saraya plutons (dated by the U/Pb method on zircon at 2074 ± 9 Ma (Gueye et al., 2007). The late deformation, dated at around 2073 Ma, was defined in Burkina Faso (Feybesse et al., 1989). It marks the end of the Eburnian event. This last magmatic activity was characterised by transcurrent tectonics accompanied by magmatism and the closure of the basin.

The closure of the Diale basin is thought to be associated with Late Deformation

phase D4 located beyond the D3 phase (CiscoE = MTZ) and associated with the Late Magmatic Phase. This late magmatic event marked by emission of rhyolites and dacites associated with a highly potassic plutonism (Mineral Plan) and garnet leucogranites represents the end of crustal thickening. In summary, the opening of the Diale back-arc-basin is related to D2 = CiscoM, while its closure could be associated to D4. A compilation of the cartographic and geophysical data available in the Dalema could situate the D4 at the level of the Faleme shear-contact (CiscoF). Diabba was formed from D2 to D4 phases. The initiation of Diale basin is related to CiscoM and its closure set along the Faleme shear-contact (CiscoF) located beyond CiscoE. The tectonic evolution of the Eburnian orogeny within Mako-Diale transition zone highlights from West to East four deformation phases : CiscoW, CiscoM, CiscoE and CiscoF respectively running for D1, D2, D3 and D4. These shears-affected contact zones, sites of intense tectonic processes and geological evolution, are sites of concentration of economic minerals such as gold for Sabadala and Sofia deposits along the CiscoW; for Massawa deposit along the CiscoE. This suggests that CiscoM, CiscoF stand as potential host structures for futures Kedougou inlier deposits.

Diabba is an epicontinental graben that forms the back-arc basin associated with Maco oceanic complex and Sesam island arc. Overall, the geodynamic evolution of the Mako-Diale transition zone located within the Kedougou-Kenieba inlier is linkable to a single magmatic event associated with tectonomagmatic episodes (**Figure 23**). The transition from Maco to Sesam would have taken place through a process of magmatic differentiation leading to the production of tholeiitic suites and calc-alkaline series.

7. Conclusion

The geological and geophysical mapping and lithostructural interpretation carried out as part of this work have shown that the transitional zone between volcanic belt and Diale basin is a non-homogeneous lithostructural framework. The highlighting of true western limite of Diale sedimentary basin (CiscoM) enables the definition of this latest architecture of transition zone between Mako volcanic belt and Diale basin. Three lithostructural domains (Maco, Sesam and Diabba) evolving to three tectonomagmatic complexes were highlighted within Kedougou-Kenieba inlier : Maco oceanic crust, Sesam Arc and Diale back-arc basin.

Maco oceanic crust volcanism is unimodal (calc-alkaline) and associated with two tholeiitic series showing distinct magmatic sources in context of volcanic arc.

Sesam arc is marked by bimodal volcanism (tholeiitic and calc-alkaline) including Morbs tholeiites and also island arc tholeiites located at the edge the continent.

In the same spirit, Diabba is marked by bimodal volcanism (tholeiitic and calc-alkaline) including continental MORBs tholeiites and MORBs or OIBs tholeiites.

Plutonic masses within Mako-Diale transition zone belong all to three (3) different magmatic sources: Maco calc-alkaline diorite, Koulountou and Tinkoto granites and tholeiitic diorite of Maco come from high-K mafic rocks, while

Tiguida granite, Diabba granodiorite and Maco tholeiitic gabbros belong to low-K mafic sources. The Dioudiokoukou granite is sourced from tonalite rocks.

The magmatic arc corresponding to Sesam is delineated to the West by the CiscoW = SSZ and to the East by CiscoM. The magmatic arc is mainly consists of volcanics (andesitic breccias or agglomerates, andesitic tuffs) reworked by garnet granitoids. The architecture of Koulountou and Tiguida garnet granites is designed using field and radiometric data. The Kedougou Kenieba inlier magmatic arc (Sesam) shows MORBs tholeiites associated with arc tholeiites and calc-alkaline series: Sesam tholeiites3 (andesitic basalt) with MORBs affinity; Sesam tholeiites4 (andesite) with MORBs affinity and arc tholeiites; these tholeiitic series are associated with the calc-alkaline Sesam serie2 (andesite, volcanosediment) and calc-alkaline metaluminous syncollisional Koulountou granite and the peraluminous, calc-alkaline and post-collisional Tiguida granite.

Magmatic formations characteristic of magmatic arc maturity are generally more evolved and rich in silica. Sesam's andesites constitute intermediate volcanics from moderate silica enriched magmas. Dacites observed are richer in silica than andesites suggesting advanced magmatic evolution. Although rhyolites, which are very silica-rich volcanic rocks often associated with the most advanced stages of magmatic arc maturation, were not identified by the geochemical analysis of the 24 samples (this does not means they are missing in the whole area), however, the emplacement of granodiorites of Koulountou and granites of Koulountou and Tiguida indicates slow crystallisation of evolved magmas. Andesites, dacites, granodiorites and granites reflect a chemical and mineralogical evolution toward a dynamic evolution of Sesam magmatic arc.

Furthermore, the back-arc sediments characteristic of magmatic arc maturity depend on specific geological conditions. The presence of volcanic sediments (volcanoclastite from the erosion of arc volcanoes including volcanic ash to lapillis tuffs), of clastic sediment (dominated by greywackes and conglomerates resulting from the erosion of arc mountains) and sediments riches in argiles (metapelites graphitic associated to variates environnements, graphitic schistes associated to high pressure and moderate temperature environnements and even fine metasediments associated to oceanic environnement of Maco) also reflect tectonic and magmatic evolution of the arc.

Acknowledgements

My Acknowledgment go to:

- M. Mohamed David Mbaye, contry manager at Barrick gold Senegal, who provided me facilities and means of locomotion for mapping and data collection.
- Professeur Papa Malick Ngom for his scientific contribution to petrology.
- Professor Alain Nicaise Kouamela and the laboratory of the UFR Earth Sciences and mineral resources of Felix Ouphouet Boigny University for their support in producing the 24 thin section samples and polished sections.
- Professors Moussa Dabo, Mababa Diagne and Doctors Serigne Sylla and Ma-

tar Ndiaye for support during thesis work.

- Mrs. Ciss Aminata Diouf, Head of the Analytical Laboratories group at Ministry of Mines and Geology, for her help in preparing rock powders for the geochemical study.
- M. Antoine de Haller of the Department of Earth Sciences at the University of Geneva, for his support in carrying out the QUEMSCAN analysis.
- M. Andrea Moscariello of the Department of Earth Sciences, University of Geneva, for kindly covering the costs of the 24 QUEMSCAN and 24 XRF samples in his departmental budget. And finally University of Lausanne for carrying out the geochemical analyses via XRF or X-ray fluorescence spectrometry.

Conflicts of Interest

The authors declare no conflicts of interest regarding the publication of this paper.

References

- Abouchami, W., Boher, M., Michard, A., & Albarede, F. (1990). A Major 2.1 Ga Event of Mafic Magmatism in West Africa: An Early Stage of Crustal Accretion. *Journal of Geophysical Research: Solid Earth*, *95*, 17605-17629.
<https://doi.org/10.1029/jb095ib11p17605>
- Agyei Duodu, J., Loh, G. K., Boamah, K. O., Baba, M., Hirdes, W., Toloczyki, M., & Davis D. W. (2009). *572 Geological Map of Ghana 1: 1,000,000; Geological Survey of Ghana, Map 1: 1M.*
- Ama Salah, I., Liegeois, J., & Pouclet, A. (1996). Evolution d'un arc insulaire océanique birimien précoce au Liptako nigérien (Sirba): Géologie, géochronologie et géochimie. *Journal of African Earth Sciences*, *22*, 235-254.
[https://doi.org/10.1016/0899-5362\(96\)00016-4](https://doi.org/10.1016/0899-5362(96)00016-4)
- Arnould, M. (1961). *Etude géologique des migmatites et des granites précambriens du nord-est de la Côte d'Ivoire et de la Haute-Volta méridionale.* Bureau de recherches géologiques et minières.
- Attoh, K., Evans, M. J., & Bickford, M. E. (2006). Geochemistry of an Ultramafic-Rodingite Rock Association in the Paleoproterozoic Dixcove Greenstone Belt, Southwestern Ghana. *Journal of African Earth Sciences*, *45*, 333-346.
<https://doi.org/10.1016/j.jafrearsci.2006.03.010>
- Baratoux, L., Metelka, V., Naba, S., Jessell, M. W., Grégoire, M., & Ganne, J. (2011). Juvenile Paleoproterozoic Crust Evolution during the Eburnean Orogeny (~2.2-2.0ga), Western Burkina Faso. *Precambrian Research*, *191*, 18-45.
<https://doi.org/10.1016/j.precamres.2011.08.010>
- Bard, J. P. (1974). Remarques à propos de l'évolution géotectonique du craton Ouest Africain. *Comptes rendus de l'Académie des Sciences*, *278*, 2405-2408.
- Barrere, J. (1967). *Le groupe précambrien de l'Amsaga entre Atar et Akjoujt (Mauritanie). Etude d'un métamorphisme profond et de ses relations avec la migmatisation.* Ph.D. Thesis.
- Bassot, J. P. (1963) *Etude géologique du Sénégal oriental et des confins guinéo-maliens.* Master's Thesis.
- Bassot, J. P. (1966). *Etude géologique du Sénégal Oriental & de ses confins Guinéo-maliens.*

https://bibliotheques.mnhn.fr/medias/detailstatic.aspx?INSTANCE=exploitation&RSC_BASE=HORIZON&RSC_DOCID=103652

- Bassot, J. P. (1987). Le complexe volcano-plutonique calco-alcali de la rivière daléma (Est Sénégal): discussion de sa signification géodynamique dans le cadre de l'orogénie eburnéenne (protérozoïque inférieur). *Journal of African Earth Sciences* (1983), 6, 505-519. [https://doi.org/10.1016/0899-5362\(87\)90091-1](https://doi.org/10.1016/0899-5362(87)90091-1)
- Bassot, J. P., & Caen-Vachette, M. (1984). Données géochronologiques nouvelles sur les granitoïdes de l'EST du Sénégal: Implication sur l'histoire du Birimien de cette région. *Géologie Africaine Tervuren* (pp. 191-209). Publisher.
- Batchelor, R. A., & Bowden, P. (1985). Petrogenetic Interpretation of Granitoid Rock Series Using Multicationic Parameters. *Chemical Geology*, 48, 43-55. [https://doi.org/10.1016/0009-2541\(85\)90034-8](https://doi.org/10.1016/0009-2541(85)90034-8)
- Beckinsale, R., Gale, N., Pankhurst, R., Macfarlane, A., Crow, M., Arthurs, J. et al. (1980). Discordant Rb-Sr and Pb-Pb Whole Rock Isochron Ages for the Archaean Basement of Sierra Leone. *Precambrian Research*, 13, 63-76. [https://doi.org/10.1016/0301-9268\(80\)90059-5](https://doi.org/10.1016/0301-9268(80)90059-5)
- Bertrand, J. M. et al. (1989). Réflexions sur la structure interne du craton Ouest-Africain au Sénégal oriental et confins guinéo-maliens. *Comptes rendus de l'Académie des Sciences*, 309, 751-756.
- Beziat, D., Bourges, F., Debat, P., Lompo, M., Martin, F., & Tollon, F. (2000). A Paleoproterozoic Ultramafic-Mafic Assemblage and Associated Volcanic Rocks of the Boromo Greenstone Belt: Fractionates Originating from Island-Arc Volcanic Activity in the West African Craton. *Precambrian Research*, 101, 25-47. [https://doi.org/10.1016/S0301-9268\(99\)00085-6](https://doi.org/10.1016/S0301-9268(99)00085-6)
- Boher, M., Abouchami, W., Michard, A., Albarede, F., & Arndt, N. T. (1992). Crustal Growth in West Africa at 2.1 Ga. *Journal of Geophysical Research: Solid Earth*, 97, 345-369. <https://doi.org/10.1029/91jb01640>
- Bonhomme, M. (1962). *Contribution à l'étude géochronologique de la plate-forme de l'Ouest Africain*. Université Clermont Auvergne.
- Cabanis, B., & Lecolle, M. (1989). Le diagramme La/10-Y/15-Nb/8: Un outil pour la discrimination des séries volcaniques et la mise en évidence des processus de mélange et/ou de contamination crustale. *Sciences de la Terre*, 309, 2023-2029.
- Camil, J., Tempier, P., & Caen Vachette, M. (1984) Schéma pétrographique, structural et chronologique des formations archéennes de la région de Man (Côte d'Ivoire). Leur rôle dans la cratonisation de l'Ouest Africain. In J. Klerkx, & J. Michot (Eds.), *Géologie Africaine* (pp. 1-10).
- Castaing, C., Billa, M., Milesi, J. P., Thiéblemont, D., Le Metour, J., Egal, E., Donzeau, M., Guerrot, C., Cocherie, E. A., Chevremont, P., Tegvey, M., Itard, Y., Zida, B., Ouédraogo, I., Koté, S., Kaboré, B. E., Ouédraogo, C., Ki, J. C., & Zunino, C. (2003). *Notice Explicative de la Carte géologique et minière du Burkina Faso à 1/1 000 000*.
- Cissokho, S. (2010). *Etude géologique du secteur de Mako (partie méridionale du super-groupe de Mako, boutonnière de Kédougou-Kéniéba, Sénégal oriental): Implications sur la diversité magmatique*. Master's Thesis, Cheikh Anta Diop University.
- Cox, K. G., et al. (1979). *The Interpretation of Igneous Rocks*. Allen and Unwin, London, 450 p. <http://dx.doi.org/10.1007/978-94-017-3373-1>
- Dabo, M., Aifa, T., Gassama, I., & Ngom, P. M. (2018). Thrust to Transpression and Transtension Tectonics during the Paleoproterozoic Evolution of the Birimian Greenstone Belt of Mako, Kédougou-Kéniéba Inlier, Eastern Senegal. *Journal of African Earth*

- Sciences*, 148, 14-29. <https://doi.org/10.1016/j.jafrearsci.2018.05.010>
- Dabo, M., Aïfa, T., Gning, I., Faye, M., Ba, M. F., & Ngom, P. M. (2017). Lithological Architecture and Petrography of the Mako Birimian Greenstone Belt, Kédougou-Kéniéba Inlier, Eastern Senegal. *Journal of African Earth Sciences*, 131, 128-144. <https://doi.org/10.1016/j.jafrearsci.2017.04.005>
- Dampare, S. B., Shibata, T., Asiedu, D. K., Okano, O., Osae, S. K. D., Atta-Peters, D. et al. (2019). Ultramafic-Mafic and Granitoids Supra-Subduction Magmatism in the Southern Ashanti Volcanic Belt, Ghana: Evidence from Geochemistry and Nd Isotopes. *Geological Journal*, 55, 2495-2531. <https://doi.org/10.1002/gj.3512>
- Dampare, S. B., Shibata, T., Asiedu, D. K., Osae, S., & Banoeng-Yakubo, B. (2008). Geochemistry of Paleoproterozoic Metavolcanic Rocks from the Southern Ashanti Volcanic Belt, Ghana: Petrogenetic and Tectonic Setting Implications. *Precambrian Research*, 162, 403-423. <https://doi.org/10.1016/j.precamres.2007.10.001>
- Dampare, S., Shibata, T., Asiedu, D., Okono, O., Manu, J., & Sakyi, P. (2009). Sr-Nd Isotopic Compositions of Paleoproterozoic Metavolcanic Rocks from the Southern Ashanti Volcanic Belt, Ghana. *Earth-Science Reviews*, 16, 9-28.
- Debat, P., Diallo, D. P., Ngom, P. M., Rollet, M., & Seyler, M. (1984). La série de Mako dans ses parties centrale et méridionale (Sénégal Oriental, Afrique de l'ouest). Précisions sur l'évolution de la série volcanosédimentaire et données géochimiques préliminaires sur les formations magmatiques post-tectoniques. *Journal of African Earth Sciences* (1983), 2, 71-79. [https://doi.org/10.1016/0899-5362\(84\)90023-x](https://doi.org/10.1016/0899-5362(84)90023-x)
- Debat, P., Diallo, D. P., Rollet, M., & Seyler, M. (1982). Mise en évidence d'une série magmatique basique atectonique dans les formations birimiennes du Sénégal oriental. *Comptes Rendus de l'Académie des Sciences*, 294, 211-213.
- Debat, P., Nikiéma, S., Mercier, A., Lompo, M., Béziat, D., Bourges, F. et al. (2003). A New Metamorphic Constraint for the Eburnean Orogeny from Paleoproterozoic Formations of the Man Shield (aribinda and Tampelga Countries, Burkina Faso). *Precambrian Research*, 123, 47-65. [https://doi.org/10.1016/s0301-9268\(03\)00046-9](https://doi.org/10.1016/s0301-9268(03)00046-9)
- Delor, C., Couëffé, R., Goujou, J. C. et al. (2010). *Notice 607 explicative de la carte géologique à 1/200 000 du Sénégal, feuille Saraya-Kédougou Est*. 608 Ministère des Mines, de l'Industrie, de l'Agro-Industrie et des PME, Direction des Mines et de la Géologie, Dakar.
- Dercourt, Gaetani, M. et al. (2000). *Atlas Peri-Tethys, Palaeogeographical Maps*. https://www.researchgate.net/publication/258505590_Atlas_Peri-Tethys_paleogeographical_maps
- Dia, A. (1988). *Caractères et significations des complexes magmatiques et métamorphiques du secteur de Sandikounda-Laminia (Nord de la boutonnière de Kédougou-Kéniéba, Est du Sénégal)*. Ph.D. Thesis, Cheikh Anta Diop University.
- Dia, A., Van Schmus, W. R., & Kröner, A. (1997). Isotopic Constraints on the Age and Formation of a Palaeoproterozoic Volcanic Arc Complex in the Kedougou Inlier, Eastern Senegal, West Africa. *Journal of African Earth Sciences*, 24, 197-213. [https://doi.org/10.1016/s0899-5362\(97\)00038-9](https://doi.org/10.1016/s0899-5362(97)00038-9)
- Diallo, D. P. (1983). *Contribution à l'étude géologique de la série du Dialé (Birimien) dans les monts Bassaris-Sénégal oriental (secteur de Bandafassi-Ibel-Ndébou-Landiéné)*. Ph.D. Thesis, Cheikh Anta Diop University.
- Diallo, D. P. (1994). *Caractérisation d'une portion de croûte d'âge protérozoïque inférieur du craton ouest africain: Cas de l'encaissant des granitoïdes dans le supergroupe de Mako (Boutonnière de Kédougou)*. *Implications géodynamiques*. Ph.D. Thesis, Cheikh Anta Diop University, 466 p.

- Diallo, D. P. (2001). Le paléovolcanisme de la bordure occidentale de la boutonnière de Kédougou, Paléoproterozoïque du Sénégal oriental: incidences géotectoniques. *Journal of African Earth Sciences*, 32, 919-940. [https://doi.org/10.1016/S0899-5362\(02\)00063-5](https://doi.org/10.1016/S0899-5362(02)00063-5)
- Diene, M., Gueye, M., Diallo, D. P., & Dia, A. (2012). Structural Evolution of a Precambrian Segment: Example of the Paleoproterozoic Formations of the Mako Belt (eastern Senegal, West Africa). *International Journal of Geosciences*, 3, 153-165. <https://doi.org/10.4236/ijg.2012.31017>
- Dioh, E. (1995). *Caractérisation, signification et origine des formations Birimiennes encaissantes du granite de Diombalou (partie septentrionale de la boutonnière de Kédougou-Sénégal oriental)*. Ph.D. Thesis, Cheikh Anta Diop University.
- Dioh, E., Béziat, D., Debat, P., Grégoire, M., & Ngom, P. M. (2006). Diversity of the Palaeoproterozoic Granitoids of the Kédougou Inlier (Eastern Sénégal): Petrographical and Geochemical Constraints. *Journal of African Earth Sciences*, 44, 351-371. <https://doi.org/10.1016/j.jafrearsci.2005.11.024>
- Dioh, E., Béziat, D., Grégoire, M., & Debat, P. (2009). Origin of Rare Earth Element Variations in Clinopyroxene from Plutonic and Associated Volcanic Rocks from the Foulde Basin, Northern Kedougou Inlier, Senegal, West Africa. *European Journal of Mineralogy*, 21, 1029-1043. <https://doi.org/10.1127/0935-1221/2009/0021-1963>
- Dupuis, D., Pons, J., & Prost, A. E. (1991). Mise en place de plutons et caractérisation de la déformation birimiène au Niger Occidental. *Comptes Rendus de l'Académie des Sciences*, 312, 769-776.
- Feybesse, J. L., Milési, J. P., Johan, V. et al. (1989). La limite Archéen-Proterozoïque d'Afrique de l'Ouest: Une zone de chevauchement antérieure à l'accident de Sassandra; l'exemple des régions d'Ondienné et de Touba (Côte d'Ivoire). *Comptes rendus de l'Académie des Sciences*, 309, 1847-1853.
- Feybesse, J., & Milési, J. (1994). The Archaean/Proterozoic Contact Zone in West Africa: A Mountain Belt of Décollement Thrusting and Folding on a Continental Margin Related to 2.1 Ga Convergence of Archaean Cratons? *Precambrian Research*, 69, 199-227. [https://doi.org/10.1016/0301-9268\(94\)90087-6](https://doi.org/10.1016/0301-9268(94)90087-6)
- Feybesse, J., Billa, M., Guerrot, C., Duguey, E., Lescuyer, J., Milesi, J. et al. (2006). The Paleoproterozoic Ghanaian Province: Geodynamic Model and Ore Controls, Including Regional Stress Modeling. *Precambrian Research*, 149, 149-196. <https://doi.org/10.1016/j.precamres.2006.06.003>
- Ganne, J., De Andrade, V., Weinberg, R. F., Vidal, O., Dubacq, B., Kagambega, N. et al. (2012). Modern-Style Plate Subduction Preserved in the Palaeoproterozoic West African Craton. *Nature Geoscience*, 5, 60-65. <https://doi.org/10.1038/ngeo1321>
- Gasquet, D., Barbey, P., Adou, M., & Paquette, J. L. (2003). Structure, Sr-Nd Isotope Geochemistry and Zircon U–pb Geochronology of the Granitoids of the Dabakala Area (Côte D'ivoire): Evidence for a 2.3 Ga Crustal Growth Event in the Palaeoproterozoic of West Africa? *Precambrian Research*, 127, 329-354. [https://doi.org/10.1016/S0301-9268\(03\)00209-2](https://doi.org/10.1016/S0301-9268(03)00209-2)
- Girard, P., Goulet, N., & Malo, M. (1998). *Synthèse des données géologiques et cartographie, 233 Amélioration et Modernisation du centre de documentation, Géologie du Mali*.
- Gozo, A., Diène, M., Diallo, D. P., Dioh, E., Gueye, M., & Ndiaye, P. M. (2015). Petrological and Structural Approach to Understanding the Mechanism of Formation and Development of Paleoproterozoic Calc-Alkaline Volcanic Rocks of West Africa's Craton: An Example of the Mako and Foulde Groups (Kedougou Inlier in Western Senegal). *International Journal of Geosciences*, 6, 675-691.

- <https://doi.org/10.4236/jjg.2015.67055>
- Gravesteyn, J. (1962). *Mission Ouassa-Sud Falémé. Rapport de fin de mission 1961 1962*. Arch. BRGM.
- Gueye, M., & Ngom, P. M. (2020). *Reviews of the Eburnean Geodynamic evolution: Case Study of the Kedougou-Kenieba Inlier (Senegal) in Bartorelli, Andrea Geocronologia e evolução tectônica do Continente Sul-Americano: A contribuição de Umberto Giuseppe Cordani/Andrea Bartorelli, Wilson Teixeira, Benjamim Bley de Brito Neves*. Solaris Edições Culturais.
- Gueye, M., Ngom, P. M., Diène, M., Thiam, Y., Siegesmund, S., Wemmer, K. et al. (2008). Intrusive Rocks and Tectono-Metamorphic Evolution of the Mako Paleoproterozoic Belt (Eastern Senegal, West Africa). *Journal of African Earth Sciences*, 50, 88-110. <https://doi.org/10.1016/j.jafrearsci.2007.09.013>
- Gueye, M., Siegesmund, S., Wemmer, K., Pawlig, S., Drobe, M., Nolte, N. et al. (2007). New Evidences for an Early Birimian Evolution in the West African Craton: An Example from the Kedougou-Kenieba Inlier, Southeast Senegal. *South African Journal of Geology*, 110, 511-534. <https://doi.org/10.2113/gssajg.110.4.511>
- Hirdes, W., & Davis, D. W. (2002). U-Pb Geochronology of Paleoproterozoic Rocks in the Southern Part of the Kedougou-Kéniéba Inlier, Senegal, West Africa: Evidence for Diachronous Accretionary Development of the Eburnean Province. *Precambrian Research*, 118, 83-99. [https://doi.org/10.1016/s0301-9268\(02\)00080-3](https://doi.org/10.1016/s0301-9268(02)00080-3)
- Hirdes, W., Davis, D. W., & Eisenlohr, B. N. (1992). Reassessment of Proterozoic Granitoid Ages in Ghana on the Basis of U/Pb Zircon and Monazite Dating. *Precambrian Research*, 56, 89-96. [https://doi.org/10.1016/0301-9268\(92\)90085-3](https://doi.org/10.1016/0301-9268(92)90085-3)
- Hirdes, W., Davis, D. W., Lüdtké, G., & Konan, G. (1996). Two Generations of Birimian (Paleoproterozoic) Volcanic Belts in Northeastern Côte D'ivoire (West Africa): Consequences for the 'birimian Controversy'. *Precambrian Research*, 80, 173-191. [https://doi.org/10.1016/s0301-9268\(96\)00011-3](https://doi.org/10.1016/s0301-9268(96)00011-3)
- Irvine, T. N., & Baragar, W. R. A. (1971). A Guide to the Chemical Classification of the Common Volcanic Rocks. *Canadian Journal of Earth Sciences*, 8, 523-548. <https://doi.org/10.1139/e71-055>
- Jensen, L. S. (1976). *A New Cation Plot for Classifying Subalkalic Volcanic Rocks*. Ontario Division Mines, Miscellaneous Paper, 66, 22 p.
- Kock, G. S., Armstrong, R. A., Siegfried, H. P., & Thomas, E. (2011). Geochronology of the Birim Supergroup of the West African Craton in the Wa-Bolé Region of West-Central Ghana: Implications for the Stratigraphic Framework. *Journal of African Earth Sciences*, 59, 1-40. <https://doi.org/10.1016/j.jafrearsci.2010.08.001>
- Koffi, K. M., Yao, K. T., Mobio, A., & Oga, Y. M. S. (2016). Apport de l'analyse multicritère à la cartographie des zones favorables à l'implantation de forages dans la région de Gagnoa (Centre-ouest de la Côte d'Ivoire). *Revue internationale de géologie, de géographie et d'écologie tropicales*, 40, 327-3441
- Kone, J., Vanderhaeghe, O., Diatta, F., Baratoux, L., Thebaud, N., Bruguier, O. et al. (2020). Source and Deposition Age of the Dialé-Daléma Metasedimentary Series (kédougou-Kéniéba Inlier, Senegal) Constrained by U-Pb Geochronology on Detrital Zircon Grains. *Journal of African Earth Sciences*, 165, Article ID: 103801. <https://doi.org/10.1016/j.jafrearsci.2020.103801>
- Labou, I. (2019). *Les complexes basiques et ultrabasiques birimiens de la ceinture de Mako (Sénégal oriental) témoins d'une évolution d'un domaine intra-océanique vers un domaine d'arc insulaire*. Master's Thesis, Université Toulouse 3—Paul Sabatier, Toulouse.
- Labou, I., Benoit, M., Baratoux, L., Grégoire, M., Ndiaye, P. M., Thebaud, N. et al. (2020).

- Petrological and Geochemical Study of Birimian Ultramafic Rocks within the West African Craton: Insights from Mako (Senegal) and Loraboué (Burkina Faso) Lherzolite/Harzburgite/Wehrlite Associations. *Journal of African Earth Sciences*, 162, Article ID: 103677. <https://doi.org/10.1016/j.jafrearsci.2019.103677>
- Lahondere, D., Thiéblemont, D., Tegye, M., Guerrot, C., & Diabate, B. (2002). First Evidence of Early Birimian (2.21 Ga) Volcanic Activity in Upper Guinea: The Volcanics and Associated Rocks of the Niani Suite. *Journal of African Earth Sciences*, 35, 417-431. [https://doi.org/10.1016/s0899-5362\(02\)00145-8](https://doi.org/10.1016/s0899-5362(02)00145-8)
- Lambert-Smith, J. S., Lawrence, D. M., Müller, W., & Treloar, P. J. (2016). Palaeotectonic Setting of the South-Eastern Kédougou-Kéniéba Inlier, West Africa: New Insights from Igneous Trace Element Geochemistry and U-Pb Zircon Ages. *Precambrian Research*, 274, 110-135. <https://doi.org/10.1016/j.precamres.2015.10.013>
- Laurent, O., Martin, H., Moyen, J. F., & Doucelance, R. (2014). The Diversity and Evolution of Late-Archean Granitoids: Evidence for the Onset of “Modern-Style” Plate Tectonics between 3.0 and 2.5ga. *Lithos*, 205, 208-235. <https://doi.org/10.1016/j.lithos.2014.06.012>
- Lawrence, D. M., Treloar, P. J., Rankin, A. H., Harbidge, P., & Holliday, J. (2013). The Geology and Mineralogy of the Loulo Mining District, Mali, West Africa: Evidence for Two Distinct Styles of Orogenic Gold Mineralization. *Economic Geology*, 108, 199-227. <https://doi.org/10.2113/econgeo.108.2.199>
- Le Bas, M. J., Le Maitre, R. W., Streckeisen, A., & Zanettin, B. (1986). A Chemical Classification of Volcanic Rocks Based on the Total Alkali-Silica Diagram. *Journal of Petrology*, 27, 745-750. <https://doi.org/10.1093/petrology/27.3.745>
- Ledru, P., Milesi, J. P., Vinchon, C., Ankrah, P., Johan, V., & Marcoux, E. (1988). Geology of the Birimian Series of Ghana. In *International Conference and Workshop on the Geology and Exploration in Ghana and in Selected Other Precambrian Terrains* (pp. 26-27).
- Ledru, P., Pons, J., Milesi, J. P., Feybesse, J. L., & Johan, V. (1991). Transcurrent Tectonics and Polycyclic Evolution in the Lower Proterozoic of Senegal-Mali. *Precambrian Research*, 50, 337-354. [https://doi.org/10.1016/0301-9268\(91\)90028-9](https://doi.org/10.1016/0301-9268(91)90028-9)
- Ledu, P., Pons, J., Milési, J. P., Dommange, A., Johan, V., Diallo, M., et al. (1989). Tectonique transcurrente et évolution polycyclique dans le birimien, protérozoïque inférieur, du Sénégal-Mali (Afrique de l'ouest). *Comptes rendus de l'Académie des Sciences*, 308, 117-122.
- Lemoine, S. (1988). *Evolution géologique de la région de Dabakala (NE Côte d'Ivoire) au protérozoïque. Possibilités d'extension au reste de la Côte d'Ivoire et du Burkina Faso: similitudes et différences, les linéaments Greenvilles-Frekessedougou et Grand Cess Nakaramandougou.*
- Lemoine, S., Tempier, P., Bassot, J. P., Caen Vachette, M., Vialette, Y., Touré, S., & Wenmenga, U. (1990). The Burkinian Orogenic Cycle, Precursor of the Eburnean Orogeny in West Africa. *Geological Journal*, 25, 171-188. <https://doi.org/10.1002/gj.3350250208>
- Leube, A., Hirdes, W., Mauer, R., & Kesse, G. O. (1990). The Early Proterozoic Birimian Supergroup of Ghana and Some Aspects of Its Associated Gold Mineralization. *Precambrian Research*, 46, 139-165. [https://doi.org/10.1016/0301-9268\(90\)90070-7](https://doi.org/10.1016/0301-9268(90)90070-7)
- Liegeois, J. P., Claessens, W., Camara, D., & Klerkx, J. (1991). Short-Lived Eburnian Orogeny in Southern Mali. Geology, Tectonics, U-Pb and Rb-Sr Geochronology. *Precambrian Research*, 50, 111-136. [https://doi.org/10.1016/0301-9268\(91\)90050-k](https://doi.org/10.1016/0301-9268(91)90050-k)
- Loh, G., & Hirdes, W. (1999). Explanatory Notes for the Geological Map of Southwest Ghana 1: 100,000 Sekondi (0402A) and Axim (0403B) Sheets. *Bulletin of the United*

- States Geological Survey*, 49, Article 149.
- Lüdtke, G., Hirdes, W., Konan, G., Kone, Y., N'da, D., Traore, Y., & Zamble, Z. (1999). Geologie de la region Haute Comoe Sud-feuilles Dabakala (2b, d et 4b, d). *Direction de la Geologie Abidjan Bulletin*, 176.
- McFarlane, C. R. M., Mavrogenes, J., Lentz, D., King, K., Allibone, A., & Holcombe, R. (2011). Geology and Intrusion-Related Affinity of the Morila Gold Mine, Southeast Mali. *Economic Geology*, 106, 727-750. <https://doi.org/10.2113/econgeo.106.5.727>
- Meschede, M. (1986). A Method of Discriminating between Different Types of Mid-Ocean Ridge Basalts and Continental Tholeiites with the Nb 1bZr 1bY Diagram. *Chemical Geology*, 56, 207-218. [https://doi.org/10.1016/0009-2541\(86\)90004-5](https://doi.org/10.1016/0009-2541(86)90004-5)
- Metelka, V. et al. (2011). Geophysical and Remote Sensing Methodologies Applied to the analysis of regolith and geology in Burkina Faso, West Africa. *Journal of African Earth Sciences*, 60, 123-134.
- Milesi, J. P., Diallo, M., Feybesse, J. L., Keïta, E., Ledru, P., Vichon, C., & Dommangeat, A. (1986). Caractérisation lithostructurale de deux ensembles successifs dans les séries birimiennes de la boutonnière de Kédougou (Mali-Sénégal) et du Niandan (Guinée): Implications géologiques. *Les rhinoceros*, 10, 113-121.
- Milesi, J. P., Feybesse, J. L., Pinna, P., Deschamps, Y., Kampunzu, H., Muhongo, S., Lesucuyer, J. L., Le Goff, E., Delor, C., Billa, M., Ralay, F., & Henry, C. (2004). Geological map of Africa 1: 10000000 SIG Afrique Project. In *20th Conference of African Geology Bureau de Recherches Géologiques et Minières*.
- Milesi, J., Ledru, P., Feybesse, J., Dommangeat, A., & Marcoux, E. (1992). Early Proterozoic Ore Deposits and Tectonics of the Birimian Orogenic Belt, West Africa. *Precambrian Research*, 58, 305-344. [https://doi.org/10.1016/0301-9268\(92\)90123-6](https://doi.org/10.1016/0301-9268(92)90123-6)
- Mission Sénégal-Soviétique de recherches minières (1972-1973). *Rapports inédits*. Dir. Mines Géol. Dakar Sénégal.
- Moussolo, J. B. (2000). *Etude du volcanisme de Baniomba dans la partie méridionale du groupe de Mako: Boutonnière de Kédougou-Kéniéba (Sénégal Oriental)*. Mémoire de DEA Université Cheikh Anta Diop, 74 p.
- Ndiaye, P. M. (1986). *Etude géologique et metallogénique de la partie septentrionale du granite de Saraya (secteur de Missira-Wassangara-Farandi) (Sénégal Oriental)*. Ph.D. Thesis, Université Cheikh Anta Diop.
- Ndiaye, P. M. (1994). *Evolution au Protérozoïque inférieur de la région Est Saraya, Supergroupe de Dialé-Daléma Sénégal Oriental: Tourmalinisation, altérations hydrothermales et minéralisations associées*. Ph.D. Thesis, Université Cheikh Anta Diop de Dakar.
- Ngom, P. M. (1985). *Contribution à l'étude de la série Birimienne de Mako dans le secteur de Sabodala (Sénégal oriental)*. Ph.D. Thesis, University Nancy I.
- Ngom, P. M. (1995). *Caractérisation de la croûte birimienne dans les parties centrale et méridionale du Supergroupe de Mako: Implications géochimiques et pétrographiques et pétro génétiques*. Ph.D. Thesis, Université Cheikh Anta Diop de Dakar.
- Ngom, P. M., Cordani, U. G., Teixeira, W., & Janasi, V. d. A. (2010). Sr and Nd Isotopic Geochemistry of the Early Ultramafic-Mafic Rocks of the Mako Bimodal Volcanic Belt of the Kedougou-Kenieba Inlier (Senegal). *Arabian Journal of Geosciences*, 3, 49-57. <https://doi.org/10.1007/s12517-009-0051-3>
- Ngom, P. M., Gueye, M., Cissokho, S., Joron, J. L., Treuil, M., & Dabo, M. (2007). Signification géodynamique des roches volcaniques dans les ceintures de roches vertes d'âge paléoprotérozoïque; Exemple de la partie méridionale du Supergroupe de Mako, boutonnière de Kédougou (Sénégal). Approche des éléments en traces. *Journal des Sciences et*

Technologies, 5, 52-71.

- Ngom, P. M., Rocci, G., Debat, P., Dia, A., Diallo, D. P., Dioh, E., & Sylla, M. (1998). *Les massifs basiques et ultrabasiques Birimiens du super-groupe de Mako (Sénégal Oriental): Pétrographie, géochimie et signification pétrogénétique*. Université Cheikh Anta Diop de Dakar.
- Oberthür, T. (1998). Age Constraints on Gold Mineralization and Paleoproterozoic Crustal Evolution in the Ashanti Belt of Southern Ghana. *Precambrian Research*, 89, 129-143. [https://doi.org/10.1016/s0301-9268\(97\)00075-2](https://doi.org/10.1016/s0301-9268(97)00075-2)
- Ouedraogo, A. (1985). *Etude de quelques unités plutoniques basiques éburnéennes dans le sillon de Bouroum Yalogo au NE du Burkina Faso*. Master's Thesis, Université de Lorraine.
- Pawlig, S., Gueye, M., Klischies, R., Schwarz, S., Wemmer, K., & Siegesmund, S. (2006). Geochemical and Sr-Nd Isotopic Data on the Birimian of the Kedougou-Kenieba Inlier (eastern Senegal): Implications on the Palaeoproterozoic Evolution of the West African Craton. *South African Journal of Geology*, 109, 411-427. <https://doi.org/10.2113/gssaig.109.3.411>
- Pearce, J. A. (1982). Trace Elements Characteristics of Lavas from Destructive Plate Boundaries. In R. S. Thorpes (Ed.), *Andesites* (pp. 525-548). Wiley.
- Pearce, J. A., & Gale, G. H. (1977). Identification of Ore-Deposition Environment from Trace-Element Geochemistry of Associated Igneous Host Rocks. *Geological Society, London, Special Publications*, 7, 14-24. <https://doi.org/10.1144/gsl.sp.1977.007.01.03>
- Pearce, J. A., Harris, N. B. W., & Tindle, A. G. (1984). Trace Element Discrimination Diagrams for the Tectonic Interpretation of Granitic Rocks. *Journal of Petrology*, 25, 956-983. <https://doi.org/10.1093/petrology/25.4.956>
- Pitra, P., Kouamelan, A. N., Ballèvre, M., & Peucat, J. (2010). Palaeoproterozoic High-Pressure Granulite Overprint of the Archean Continental Crust: Evidence for Homogeneous Crustal Thickening (man Rise, Ivory Coast). *Journal of Metamorphic Geology*, 28, 41-58. <https://doi.org/10.1111/j.1525-1314.2009.00852.x>
- Pons, J., Barbey, P., Dupuis, D., & Léger, J. M. (1995). Mechanisms of Pluton Emplacement and Structural Evolution of a 2.1 Ga Juvenile Continental Crust: The Birimian of South-western Niger. *Precambrian Research*, 70, 281-301. [https://doi.org/10.1016/0301-9268\(94\)00048-v](https://doi.org/10.1016/0301-9268(94)00048-v)
- Poulet, A., Doumbia, S., & Vidal, M. (2006). Geodynamic Setting of the Birimian Volcanism in Central Ivory Coast (Western Africa) and Its Place in the Palaeoproterozoic Evolution of the Man Shield. *Bulletin de la Société Géologique de France*, 177, 105-121. <https://doi.org/10.2113/gssgfbull.177.2.105>
- Poulet, A., Vidal, M., Delor, C., Siméon, Y., & Alric, G. (1996). Le volcanisme birimien du nord-est de la Côte-d'Ivoire, mise en évidence de deux phases volcano-tectoniques distinctes dans l'évolution géodynamique du Paléoprotérozoïque. *Bulletin de la Société Géologique de France*, 167, 529-541.
- Ratomaharo, S., Demange, M., Fontailles, M., Joron, J. L., & Treuil, M. (1988). La serie birimienne de Perkoa (Burkina-Faso): Géochimie et mineralogie: Interpretation lithostratigraphique: Consequences sur l'interpretation geodynamique du Birrimien. *Comptes rendus de l'Académie des Sciences*, 307, 2033-2040.
- Roques, M. (1948). Le Precambrien de l'Afrique occidentale française. *Bulletin de la Société Géologique de France*, 5, 589-628. <https://doi.org/10.2113/gssgfbull.s5-xviii.8-9.589>
- Sangaré, A. (2008). *Les roches ultramafiques et mafiques Paléoprotérozoïques de la ceinture de roches vertes de Kadiolo (Mali). Pétrologie, évolution et ressources minérales*

- associées. *Mémoire de fin d'études*. Master's Thesis, Sidi Mohamed Ben Abdellah University.
- Shand, S. J. (1943). The Sarmatian Crustal Segment: Precambrian Correlation between the Voronezh Massif and the Ukrainian Shield across the Dniepr-Donets Aulacogen. *Tectonophysics*, 268, 109-125. [https://doi.org/10.1016/s0040-1951\(96\)00227-2](https://doi.org/10.1016/s0040-1951(96)00227-2)
- Sow, D. (2004). *Etude des paramètres lithostratigraphiques et géomorphologiques dans le contrôle de la minéralisation aurifère du corridor de Tombo-sofia, Sénégal oriental*.
- Sylvester, P. J., & Attah, K. (1992). Lithostratigraphy and Composition of 2.1 Ga Greenstone Belts of the West African Craton and Their Bearing on Crustal Evolution and the Archean-Proterozoic Boundary. *The Journal of Geology*, 100, 377-393. <https://doi.org/10.1086/629593>
- Tagini (1959). *Compte rendu de la campagne 1958-1959*. Bureau de Recherches Géologiques et Minières.
- Tempier, P. (1986). Le Burkinien: Cycle orogénique majeur du Protérozoïque inférieur en Afrique de l'Ouest. *Publication occasionnelle-Centre international pour la formation et les échanges géologiques*, 10, 17-23.
- Theveniaut, H., Ndiaye, P. M., Buscail, F., Coueffe, R., Delor, C., Fullgraf, T., & Goujou, J. C. (2010). *Notice explicative de la carte géologique du Sénégal oriental à 1/500000*. Ministère des Mines, de l'industrie de l'agro-industrie et des PME, Direction des mines et de la géologie.
- Vachette, M., Rocci, G., Souguy, J., Caron, J. P., Marchand, J., & Tempier, C. (1973). Ages radiométriques Rb/Sr, de 2000 à 1700 Ma, des séries métamorphiques et granites intrusifs Précambriens de la partie N et NE de la dorsale Réguibat (Mauritanie). *Journal of African Earth Sciences*, 12, 345-356.
- Vidal, M., Delor, C., Pouclet, A., Siméon, Y., & Alric, G. (1996). Evolution géodynamique de l'Afrique de l'Ouest entre 2.2 Ga et 2 Ga: le style archéen des ceintures vertes et des ensembles sédimentaires Birimiens du Nord-Est de la Côte-d'Ivoire. *Bulletin de la Société Géologique de France*, 167, 307-319.
- Vidal, M., Gumiaux, C., Cagnard, F., Pouclet, A., Ouattara, G., & Pichon, M. (2009). Evolution of a Paleoproterozoic "weak Type" Orogeny in the West African Craton (Ivory Coast). *Tectonophysics*, 477, 145-159. <https://doi.org/10.1016/j.tecto.2009.02.010>
- Zonou, S. (1987). *Les formations leptino-amphibolitiques et le complexe volcanique et volcano-sédimentaire du Protérozoïque inférieur de Bouroum-nord (Burkina-Faso, Afrique de l'Ouest)*. Etude pétrographique, géochimique, approche pétrogénétique et évolution géodynamique. Ph.D. Thesis, Université de Lorraine.